sustainability

MDPI

Article

Sustainability Enhancement through High-Dose Recycled Tire Steel Fibers in Concrete: Experimental Insights and Practical Applications

Asad Zia [1,2], Pu Zhang [1,*], Ivan Holly [2] and Jaroslav Prokop [2]

1 School of Water Conservancy and Civil Engineering, Zhengzhou University, Zhengzhou 450001, China; xzia@stuba.sk or asadzia005@gs.zzu.edu.cn

2 Department of Concrete Structures and Bridges, Slovak University of Technology, 811 05 Bratislava, Slovakia; ivan.holly@stuba.sk (I.H.); jaroslav.prokop@stuba.sk (J.P.)

* Correspondence: zhpu@zzu.edu.cn

Abstract: This study investigates the viability of incorporating high doses of recycled tire steel fibers (RSFs) in concrete to enhance sustainability. To address this, RSFs are incorporated at volume fractions ranging from 1% to 1.75% in the concrete mixture. The study evaluates various performance parameters, including workability, elastic modulus, compressive strength (CS), split tensile strength (SS), flexural strength (FS), linear shrinkage (LS), and water absorption (WA). Results show a 10% improvement in SS and a 4% improvement in FS compared to plain concrete (0RFRC). Additionally, RSF-reinforced concrete (RFRC) exhibits a maximum 15% reduction in LS. Water absorption slightly increases, and adverse effects on CS and workability are noted with high RSF doses. RFRC can impact the cost of rigid pavements due to reduced depth requirements. Disposing of discarded tires and their by-products has emerged as a substantial environmental challenge, obstructing progress toward achieving net-zero targets. As a sustainable solution, this study explores the potential utilization of secondary materials derived from discarded tires within the construction industry. In conclusion, this research highlights the significant potential of utilizing RSFs to enhance the sustainability of infrastructure and contribute to more eco-friendly construction practices.

Keywords: waste recycling; fiber-reinforced concrete; waste tires; sustainability; durable materials; concrete pavements

Citation: Zia, A.; Zhang, P.; Holly, I.; Prokop, J. Sustainability Enhancement through High-Dose Recycled Tire Steel Fibers in Concrete: Experimental Insights and Practical Applications. *Sustainability* **2023**, *15*, 15760. https://doi.org/10.3390/su152215760

Academic Editor: Edoardo Bocci

Received: 6 October 2023
Revised: 16 October 2023
Accepted: 18 October 2023
Published: 8 November 2023

1. Introduction

One of the primary objectives of the United Nations is to promote environmental sustainability through waste recycling. However, certain waste materials pose significant challenges when transforming them into useful resources. Solid waste materials that cannot be efficiently recycled are often repurposed and incorporated into different materials and products, such as utilizing anti-stripping-treated waste ceramic in superpave asphalt mixtures [1], silane-treated waste glass powder in concrete pavement [2], bagasse ash in asphalt concrete pavements [3], water treatment sludge and stone dust in concrete [4], and recycled waste glass in ultra-high-performance concrete [5]. One example of a major solid pollutant is discarded tires, which can take up to 100 years to degrade when exposed to the open air [6–8]. Therefore, finding effective techniques to reuse and repurpose waste tires and their components is paramount.

Considerable research has been dedicated to the reuse and recycling of rubber obtained from discarded tires [9]. In Europe, an optimized approach to managing used tires, based on the principle of extended producer responsibility, has gained popularity for its effectiveness [10]. Although the recovery rate for scrap tires in Europe and the United States is approximately 90% [11], it is predicted that by 2030, there will be up to 5 billion end-of-life tires (ELTs) in landfills and stockpiles globally [12]. It was estimated that China alone would produce 20 million metric tons of tires in 2020 [13]. Hence, other industries, including the construction sector, must contribute to the utilization of discarded tires.

The European Tyre and Rubber Manufacturers' Association (ETRMA) stated that the burden of waste tires is increasing in Slovakia, where no waste tires are currently being used for backfilling, public works, or civil engineering purposes [14]. The amount of steel fiber that can be recovered from waste tires varies depending on the type of tire, with steel accounting for approximately 10–15% of lightweight vehicles and 21–25% of trucks [12,15]. Steel cords and fibers constitute the third-largest component by weight in a tire, making up 15–17 percent of its total weight [16].

Various studies have explored the use of different types of fibers to enhance the mechanical properties of cement composites. However, industrial fibers of all types come at a cost, with natural fibers generally being more affordable than their industrial counterparts. For instance, the incorporation of natural fibers like jute and wheat straw fibers has been shown to improve the mechanical properties of concrete [17–19]. However, natural fibers have limitations in terms of biodegradability, bond strength with concrete, and decomposition over time. In some cases, additional treatments are required to improve the bond between natural fibers and cement composites, as demonstrated by Farooqi and Ali's study on pre-treated wheat straw fibers [20].

Furthermore, chemical treatments can enhance the bond between natural fibers and cement composites in the short term but may negatively impact the long-term performance of the fibers. Natural fibers, such as jute and wheat straw fibers, also tend to absorb water, which can accelerate their degradation and lead to water seepage in concrete [17,18]. Similarly, studies involving coconut fibers (shell and husk) have shown high water absorption compared to plastic or steel fibers [21–23]. On the other hand, natural resources are also depleting and come at a cost now; hence, natural fibers also have considerable cost, and additional treatment required for increasing their bond and other properties enhances their cost further. Therefore, natural fibers may not always be the optimal choice for achieving reliable long-term results compared to non-biodegradable fibers.

On the other hand, certain artificial fibers, like glass fibers, are not chemically stable when in contact with cement and other chemicals. By replacing industrially produced steel or other types of fibers with waste fibers obtained from discarded tires, energy consumption, greenhouse gas emissions, and costs can be reduced [24]. Qin and Kaewunruen [25] stated that the average cost of industrial steel fibers (ISF) is over five times that of recycled waste tire steel fibers (RSFs). The results show that using RSF replacements for ISF has a considerable positive impact on the economy and the environment. Additionally, the social function of RSF cannot be disregarded. Waste tires (and their components) cause severe environmental issues [26,27]. The RSF performs equally to the ISF in improving concrete split and flexure strengths, according to a previous study [28,29]. A comprehensive review by Zia et al. [30] further supports the potential use of RSFs in cement composites, highlighting significant enhancements in mechanical strengths.

However, it is worth noting that the available database of experimental studies related to RSF-incorporated concrete (RFRC) is still insufficient to draw conclusive findings regarding the optimal content of RSFs for desired characteristics [31–35]. Particularly, the majority of investigations [36–39] lack the experimental evaluation of RFRC for linear shrinkage and water absorption, thus neglecting the essential aspect of RFRC's durability. Therefore, there is a need to extensively test the mechanical and durability properties of RFRC to enhance the existing experimental database. Furthermore, the literature review indicates a lack of information on energy absorption and toughness of RFRC for all mechanical strengths. Consequently, various properties and aspects are missing in the current studies regarding the experimental properties of RSF-reinforced concrete, as shown in Table 1. The strength properties of RSFRCs have indeed been evaluated in the previous studies, but as per the limited literature review of the authors, the mechanical strengths, elastic modulus, capacity to absorb water, and linear shrinkage have not all been reported so far for the same mix and concrete type in one study. In addition, the influence of high doses of RSFs on the concrete properties has also not been explored extensively. Gul et al. [40] investigated the properties of concrete incorporating meticulously selected RSFs, measuring 100 mm in length and 0.939 mm in thickness. However, this study did not provide data on essential characteristics such as the elastic modulus (EM), water absorption (WA), and linear shrinkage (LS). Similarly, Rossli and Ibrahim [36] explored the effects of RSFs with dimensions of 60 mm in length and 0.80 mm in thickness on various mechanical properties.

Nevertheless, this research did not report critical parameters like EM, WA, and LS. In the work of Leone et al. [41], concrete containing a low percentage of raw RSFs (ranging from 0.3% to 0.46% by volume of concrete) exhibited a noTable 10% decrease in compressive strength (CS) and a 3% reduction in split tensile strength (SS). However, critical properties such as bending strength (BS), EM, WA, and LS were not subject to assessment. Caggiano et al. [42] delved into the influence of RSFs measuring 26.17 mm in length and 0.25 mm in thickness on concrete properties. While their study revealed a 3% decrease in CS, data pertaining to significant attributes including EM, SS, WA, and LS, were not included. Pawelska-Mazur and Kaszynska [24] and Samarakoon et al. [43] both explored the potential of raw RSFs to enhance concrete properties. However, their assessments did not address crucial factors such as EM, WA, and LS. Among the limited existing studies, Skarżyński and Suchorzewski [44] and Zia et al. [45] stand out as the sole research efforts that examined the impact of 0.50% to 0.75% of raw RSFs on concrete linear shrinkage (LS). The findings of Skarżyński and Suchorzewski [44] indicated an increase in LS attributed to the incorporation of RSFs.

In contrast, Zia et al. [45] reported a decrease in LS at an RSF dosage of 0.75%, but they observed an increasing trend in LS with a gradual rise in RSF dosage. Nevertheless, further research is essential to validate the definitive influence of raw RSFs on controlling LS. It is also noteworthy that the investigation of water absorption (WA) is a relatively rare occurrence within the available database, with only a few studies, including those by Shah et al. [46] and Akhtar et al. [47], exploring this characteristic.

Furthermore, the majority of the studies in this field have predominantly investigated the influence of low dosages of RSFs. For instance, Rossli and Ibrahim [36] employed RSFs in concentrations ranging from 0.20% to 1% by volume of concrete, Leone et al. [41] used 0.46%, Caggiano et al. [42] 0.75%, Vistos et al. [28] 0.50%, Samarakoon et al. [43] examined 0.50% and 1%, Skarżyński and Suchorzewski [44] investigated 0.50%, Aiello et al. [48] considered dosages between 0.13% to 0.26%, Chen et al. [37] explored the range from 0.50% to 1.25%, and Dorr et al. [49] studied the effect of 0.50% RSFs. Hence, there exists a critical need to comprehensively evaluate the effectiveness of high doses of RSFs to determine their potential implications on the behavior of concrete.

Moreover, it is crucial to underscore that the majority of existing studies have focused on the influence of RSFs in a meticulously separated and purified form. However, commercially available RSFs are typically presented in a raw state, characterized by varying sizes and the presence of a minute rubber content. This divergence emphasizes the utmost significance of assessing the impact of RSFs on a comprehensive range of mechanical properties and durability-defining attributes, including LS and WA, within the context of the same concrete type.

To address this gap, the current research goal is to assess the strength and durability characteristics of RSF concrete (RFRC). Different dosages of RSFs are examined using locally available materials, including RSFs and the local concrete C20/25 from Bratislava, Slovakia. This study is part of an extensive experimental program where high quantities of RSFs, extending from 1% to 1.75% by concrete volume, are included. Approximately one percent of polyester, small steel fibers, and rubber fragments were included in the mix of the fibers used in this study. The mechanical properties, such as the elastic modulus, compressive strength, split tensile strength, and flexural strength, are thoroughly evaluated. Additionally, parameters such as densities, slumps, energy absorption, toughness, capacity to absorb water by immersion, and change in length due to shrinkage are measured as well.

Table 1. Missing properties in the previous studies.

Authors	Missing in the Previous Studies	
	Strength Properties	Other Properties
Gul et al. [40]	EM	WA, LS
Rossli and Ibrahim [36]	EM	WA, LS
Leone et al. [41]	EM, BS	WA, LS
Caggiano et al. [42]	EM, SS	WA, LS
Pawelska-Mazur and Kaszynska [24]	EM, BS	WA, LS
Samarakoon et al. [43]	EM	WA, LS
Skarżyński and Suchorzewski [44]	EM	WA
Aiello et al. [48]	EM, BS	WA, LS
Chen et al. [37]	EM, SS, BS	WA, LS
Shah et al. [46]	EM, SS	LS
Siraj and Kedir [50]	SS, EM	WA, LS
Köroğlu [51]	EM	WA, LS
Abdul Awal et al. [52]	EM	WA, LS
Centonze et al. [53]	EM, SS, BS	WA, LS
Akhtar et al. [47]	EM	LS
Younis [54]	EM	WA, LS
Suleman et al. [55]	EM, SS	WA, LS
Peng et al. [56]	EM, BS	WA, LS

EM = elastic modulus, SS = split tensile strength, BS = bending strength, WA = water absorption, LS = linear shrinkage.

2. Research Gap

The existing literature on recycled tire steel fiber-reinforced concrete (RFRC) fails to provide adequate support for practical applications of RFRC within the construction industry. Many critical aspects of RFRC experimental testing remain unexplored. These include evaluating the modulus of elasticity, assessing durability-related properties such as shrinkage and water absorption, and understanding how high percentages of RSFs affect energy absorption and post-crack behavior. The current database lacks the essential information required to determine the optimized content of RSFs for specific civil engineering applications. Furthermore, evaluating locally available RSFs from Bratislava, Slovakia, is essential to promote their effective utilization in concrete at the local level. To address these research gaps, this study aims to:

Evaluate strength properties: conduct comprehensive assessments of the strength characteristics of concrete containing high volumes of recycled tire steel fibers (RSFs) to enhance the understanding of its mechanical behavior.

Analyze durability-defining properties: investigate crucial durability parameters, such as shrinkage and water absorption, to comprehend how RSFs impact the durability of RFRC.

Assess energy absorption: study the capacity of RFRC to absorb energy and its toughness characteristics, particularly when incorporating more than 1% RSFs by volume fraction.

Enhance sustainability: explore the effectiveness of RSFs in improving the sustainability of reduced-size concrete pavements.

By expanding the current database through these objectives, this research aims to provide valuable insights for future studies and engineers concerning the utilization of RSFs in concrete. This study also endeavors to enhance the understanding of the cracking behavior, toughness, and energy absorption of RFRC when incorporating high percentages of RSFs, making significant strides toward more sustainable and durable construction materials.

3. Experiments and Materials

3.1. Concrete and Ingredients

3.1.1. Concrete

In the current study, the local concrete of Bratislava was considered. The dry concrete C20/25 of Cemix Betón, available in the ready-mixed form [57], was chosen. Detailed information about the concrete can be found at [57]. Dry ready-mixed concrete was chosen for this study because it is commonly used in construction projects. This choice reflects real-world applications and ensures the relevance of our findings to practical construction scenarios. Moreover, the locally available dry ready-mixed concrete was utilized to align with the objective of the current study, which is to encourage the local adoption of RSFs in construction practices.

3.1.2. Recycled Tire Steel Fibers

The EN 14889-1:2006 [58] compliant recycled tire steel fibers (RSFs) were utilized. A small amount of rubber particles and polyester fibers were present in the RSFs used in this study. The fibers' dimensions and tensile strengths differed randomly. Figure 1 provides a photograph of the RSFs used. Statistical analysis, as conducted in the research by Zia et al. [45] determined the frequency distribution of different fiber aspects.

Figure 1. Steel fibers recovered from recycled tires.

The RSFs had diameters ranging from above 0.05 mm to less than 1.882 mm, with 5.49% having diameters larger than 0.80 mm. The majority of the RSFs (31.5%) fell within the length range of 10.5 to 13.4 mm. The RSFs had an average strength of tensile of 2459 MPa. The fibers were used in their raw form, as it was expected that approximately 1% of impurities would not adversely affect the concrete's characteristics when incorporating a high dose of RSFs.

Moreover, previous research has indicated that rubber and RSFs can enhance impact resistance [29]. Additionally, rubber particles adhered to steel fibers do not contribute to increased corrosion, possibly due to the rubber's ability to block water and chlorides [59]. Considering the minimal negative impact of the small amount of rubber and polyester fibers, they were retained in the RSFs. This approach helps reduce costs associated with processing the RSFs, as rubber constitutes a significant portion of the waste material. Furthermore, previous studies have shown that waste polyester fibers can improve the strength properties of concrete [60].

3.2. Casting Procedures

The casting procedures followed the method described in previous research [45]. A traditional concrete mixer was used for preparing concrete. To produce 0RFRCs, water and dry concrete were added to the mixer. The 0RFRC was tested for slump before being poured into molds.

The preparation of RSF mixtures (RFRC) began by placing the dry concrete into the mixer drum, followed by the addition of 75% of the water. During the initial mixing stage, the fibers were gradually incorporated into the mixture. To ensure the even distribution of RSFs, an initial step involved separating them, since these fibers tend to clump together due to variations in size and shape. Rather than adding all of the RSFs at once, a controlled technique was employed. Small portions of the fibers were methodically introduced into the mixer. These portions were gently dispersed over the concrete surface during the mixing process until the required amount of RSFs was reached. This gradual introduction of fibers was implemented to prevent any clumping or balling effects during the concrete mixing procedure. In the final step, the remaining 25% of water was added, and the mixtures were thoroughly mixed. Slump tests were conducted for the RFRCs at this stage, and the mixtures were then poured into molds. The RFRCs were tested using the same techniques as the 0RFRCs, with compaction performed following the ASTM-recommended method. All samples were cured in water tanks before undergoing testing.

3.3. Specimens and Testing Procedure

Specimens are prepared following the size requirements outlined in ASTM standards. Each property was tested using three samples, except for the water absorption test, which included two samples. An average of two readings were taken to represent the water absorption. Other researchers also reported results by taking an average of two readings; even the average of crack length was presented [61]. Research into ASTM C39 [62] and ASTM C1585 [63] also supported our use of the average of two. Specimens were labeled with specific symbols to denote the property being tested, with numbers representing the percentage of RSFs added by volume proportion of concrete (1%, 1.25%, 1.50%, and 1.75%). The specimens were indicated by labels of C for compressive strength, S for split tensile strength and F for flexure strength, and numbers 1, 2, and 3 defined the sample symbol for each specimen. The numbers 1, 12, 15, and 17 written before the RFRC represent the 1%, 1.25%, 1.50%, and 1.75% of RSFs included by the volume proportion of the mixture. The summary of tests performed, including the specimen type and size, along with ASTM standards, is demonstrated in Table 2.

Table 2. Details of standards, specimens, and tests.

S. No	Test	Specimen		Specification (ASTM Code)	Ref.
		Shape	Size		
1	Slump	Cone	200 × 100 × 300 mm	ASTM C143/C143 M-20	[64]
2	Density	Cube	150 × 150 × 150 mm	ASTM C642-13	[65]
3	Elastic modulus	Cylinder	150 × 300 mm	EN 12390-13	[66]
4	Compressive	Cylinder	150 × 300 mm	ASTM C39/C39 M-21	[67]
5	Indirect tensile	Cylinder	150 × 300 mm	ASTM C496/C496 M-17	[68]
6	Flexure	Prism	400 × 100 × 100 mm	ASTM C78/C78 M-16	[69]
7	Water absorption	Cube	150 × 150 × 150 mm	ASTM C642-13	[65]
8	Linear shrinkage	Prism	400 × 100 × 100 mm	ASTM C157/C157 M-08	[70]

The ASTM standards were followed for testing the specimens except for the elastic modulus, computed according to EN 12390-13 [66]. For strength properties, the tests included determining behavior, energies, and indices of toughness. The linear shrinkage test followed a modified method based on ASTM C157/C157 M-08, with the specimens being the standard prism size approved for bending strength following ASTM C78/C78

M-16. The baseline reading was taken subsequent to 12 h of mixing concrete with water to account for length changes during the early stage, as conducted by Khajehdehi et al. [71].

4. Findings and Evaluation

4.1. Workability and Mass

Table 3 demonstrates the slump test results. RFRCs showed less slumps than 0RFRC. The decrease in the slump for RFRCs can be attributed to the interlocking and restraint action of the fibers. A significant reduction in slump was observed for 1RFRC, 12RFRC, 15RFRC, and 17RFRC, with a 95 mm drop compared to 0RFRC. The slumps of these RFRCs were 79% lower than that of 0RFRC. The inclusion of RSFs resulted in a marked decrease in slump values. Consequently, it can be inferred that in the case of RFRCs, the use of admixtures might be necessary to attain the same level of workability as plain concrete with an equivalent mix design. However, RSFs above 1% do not further reduce the slump of the concrete. This is consistent with previous research that has reported a decrease in workability when RSFs are incorporated in concrete compared to 0RFRC [31,43].

Table 3. Slumps and densities.

Batch	Slump		Density	
	Value (mm)	Percent Comparison (%)	Value (kg/m^3)	Percent Comparison (%)
0RFRC	120	100	1968.8	100
1RFRC	25	21	1964.1	100
12RFRC	25	21	1964.2	100
15RFRC	25	21	1939.2	98
17RFRC	25	21	1971.1	100

Table 3 presents the densities of the hardened specimens. A maximum density of 1971.1 kg/m^3 was noted for 17RFRC. Compared to 0RFRC, the densities of 1RFRC, 12RFRC, and 17RFRC showed no significant change. However, a slight decrease of 2% was observed for 15RFRC. The presence of polyester and rubber in larger quantities, which have lower densities, could contribute to this slight decline. Previous studies have also reported that the density of RFRCs may exhibit slight variations [41].

4.2. Water Absorption and Linear Shrinkage

Water absorption (WA) helps to assess the concrete's durability and porosity. The water absorption test results are illustrated in Table 4. The outcomes of the water absorption test revealed that the RFRC samples (1RFRC, 12RFRC, 15RFRC, and 17RFRC) exhibited slightly higher water absorption compared to the control sample (0RFRC). This increase in water absorption ranged from 1.5% to 2%, with an increase in the percentage of RSFs. This can be attributed to the presence of RSFs, which may introduce additional pathways for water ingress into the concrete matrix. The water absorption of RFRC slightly exceeded that of plain concrete (PC) due to the higher porosity resulting from the elevated RSF content. This high RSF dosage limited optimal compaction in RFRC. A similar trend was observed in nylon fiber-reinforced concrete (NFRC), as noted by Zia et al. [17,72], where its water absorption was slightly higher than that of PC due to the increased porosity resulting from the substantial presence of nylon fibers. This abundance of fibers in NFRC hindered effective compaction.

Table 4. Water absorption and linear shrinkage test results.

Property	Type of Concrete				
	0RFRC	**1RFRC**	**12RFRC**	**15RFRC**	**17RFRC**
WA (%)	7.0	8.5	8.6	8.8	9.0
WA-CoV (%)	0.40	5.73	10.10	8.85	5.97
LS (%)	0.0165	0.0140	0.0165	0.0173	0.0175
LS-CoV (%)	0.00	4.51	30	7.26	8.08

Conversely, in the case of polypropylene fiber-reinforced concrete (PPFRC), reduced water absorption was observed compared to plain concrete. This reduction was associated with the presence of a suitable amount of fibers, which did not impede compaction, in contrast to NFRC. Thus, it can be inferred that the addition of fibers with negligible water absorption characteristics to concrete can significantly reduce capillary porosity and conductivity among pores if incorporated in an amount that does not hinder compaction due to increased heterogeneity [73,74]. In our study, a similar phenomenon occurred: an increase in fiber dosage increased heterogeneity and porosity within the mixture, leading to reduced compaction and, consequently, significantly increased water absorption.

Table 4 displays the linear shrinkage (LS) and corresponding coefficients of variation (CoV). The LS results indicated that 1RFRC exhibited a slightly lower linear shrinkage compared to 0RFRC, with a reduction of 0.0025%. However, for 12RFRC, 15RFRC, and 17RFRC, a slight increase in linear shrinkage was observed, ranging from 0.008% to 0.01%. This phenomenon can be attributed to the abundance of RSFs (1.25% to 1.75%), which may have compromised the uniformity of concrete, subsequently affecting its drying characteristics and contributing to an increased degree of shrinkage in the concrete. Similar findings regarding increased linear shrinkage due to the inclusion of thick fibers and an excessive amount of fibers, surpassing optimized dosages, have also been reported in previous studies [44,75].

In conclusion, the inclusion of RSFs in concrete resulted in a slight increase in water absorption and minor variations in linear shrinkage. These findings suggest that the presence of RSFs may influence the concrete's porosity and drying characteristics. However, the observed changes in water absorption and linear shrinkage were within acceptable ranges and are not expected to significantly impact the overall performance and durability of the RFRC. Further investigations are warranted to study the long-term effects and potential mitigation measures for these properties in RFRC.

Figure 2 provides a comparison of the results obtained from the water absorption test. The water absorption of RFRC samples (1RFRC, 12RFRC, 15RFRC, and 17RFRC) is shown to be higher compared to 0RFRC.

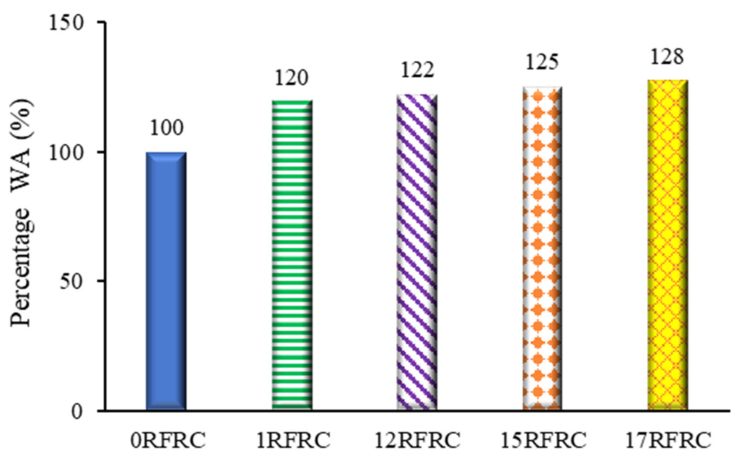

Figure 2. Percentage values of water absorption.

The water absorption increased by 20%, 22%, 25%, and 28% for 1RFRC, 12RFRC, 15RFRC, and 17RFRC, respectively, in comparison to 0RFRC. It is evident that 0RFRC exhibited the lowest water absorption among all the investigated materials. The higher water absorption in RFRC can be attributed to the less compacted nature of the RFRC specimens compared to 0RFRC. The introduction of RSFs into the concrete mix leads to increased heterogeneity, which can result in higher water absorption. By optimizing the fiber content and improving compaction through advanced techniques, it is possible to reduce water absorption. Additionally, the presence of polyester in the RSF blend may contribute to increased water absorption. It is likely that using polyester-free RSFs would reduce the water absorption in RFRC.

The progression of linear shrinkage over time is presented in Figure 3. It can be observed that the constraining effect of the optimized dose of fibers increased gradually over time. On the 28th day, the lowest LS is noted for specimens incorporating 1% of fibers. Compared to the LS of zero-fiber concrete, increased LS are noted at 1.5% and 1.7% of fibers.

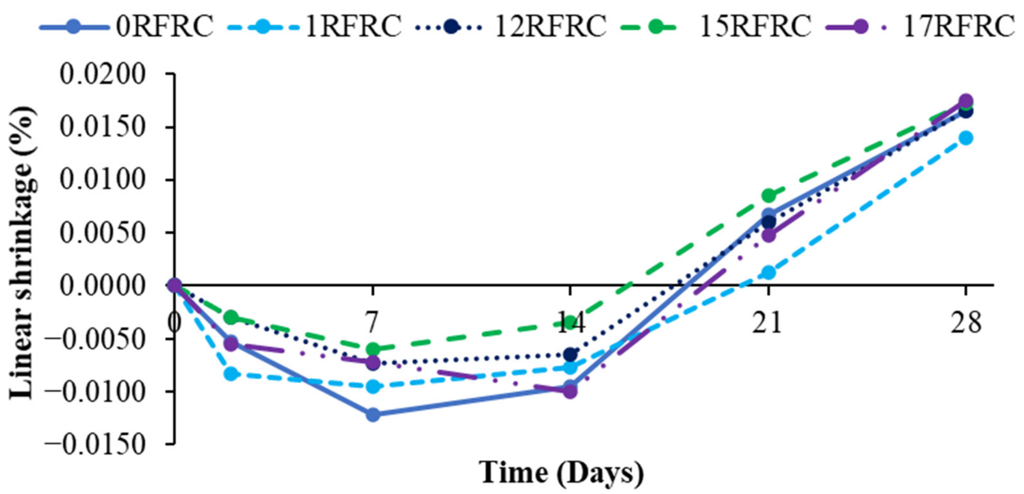

Figure 3. Evolution of linear shrinkage over time.

The linear shrinkage of specimens is represented as a percentage comparison in Figure 4. The LS of 15RFRC and 17RFRC increased by 5% and 6%, respectively, compared to 0RFRC. However, 1RFRC exhibited the best performance in limiting linear shrinkage, demonstrating 15% lower LS than 0RFRC. The LS for 12RFRC was the same as that of 0RFRC. The high dose of fibers (1%) effectively maintained the connectivity of RFRCs without compromising the uniformity of concrete and its ability to absorb tensile stresses. Previous studies have also reported a reduction in linear shrinkage with the incorporation of low dosages of industrial steel, polypropylene fibers, and recycled steel fibers [76,77]. The current research provides insights into the influence of high doses of RSFs on the linear shrinkage of concrete.

This demonstrates that RSF inclusion can effectively manage linear shrinkage up to a certain fiber proportion. However, exceeding this threshold results in increased linear shrinkage compared to plain concrete. This research highlights the crucial balance needed when incorporating RSFs to control linear shrinkage effectively. Additionally, plain concrete specimens exhibit lesser resistance to length changes compared to RFRC. Therefore, 1RFRC with reduced LS has demonstrated its potential to effectively restrict tensile cracks caused by external factors. It can be inferred that adding a 1% content of RSFs can significantly enhance the performance of concrete structures in maritime and other environments prone to tensile cracking due to extreme weather conditions.

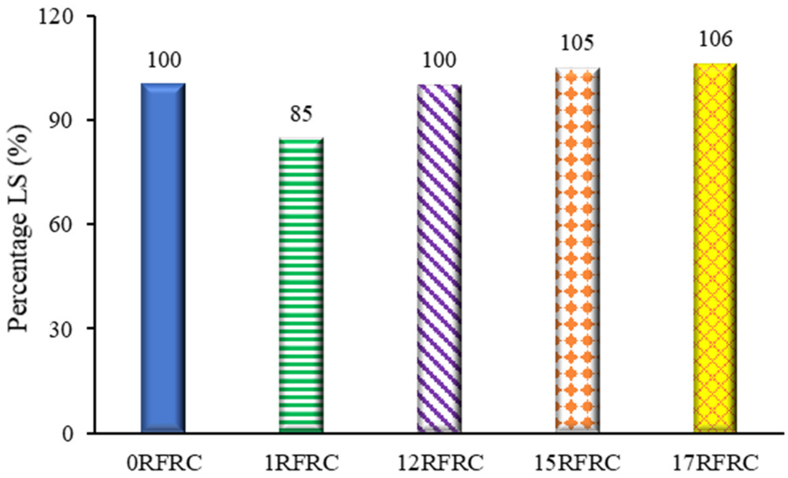

Figure 4. Percentage values of linear shrinkage.

4.3. Experimental Elastic Modulus (EM)

The European standard EN 12390-13 was used to determine the experimental value of the elastic modulus of specimens (EM). Table 5 presents the EM values for different RFRC samples, along with the corresponding coefficients of variation (CoV). The CoV values indicate the level of consistency among the three readings taken for each sample, with a maximum CoV of 7% observed, indicating good coherence among the measurements.

Table 5. Specimens' elastic modulus.

Characteristic	Type of Mixture				
	0RFRC	**1RFRC**	**12RFRC**	**15RFRC**	**17RFRC**
EM (MPa)	23,641	18,440	18,533	18,647	18,907
CoV (%)	3	4	5	7	5

The EM values for the RFRC samples exhibit variations compared to 0RFRC. The incorporation of recycled tire steel fibers leads to a reduction in the elastic modulus. The EM values for 1RFRC, 12RFRC, 15RFRC, and 17RFRC are 18,440 MPa, 18,533 MPa, 18,647 MPa, and 18,907 MPa, respectively, which are lower than the EM of 0RFRC (23,641 MPa).

Figure 5 provides a graphical representation of the percentage comparison of the EM values. It can be observed that 1RFRC exhibited a decline of 22% in EM, while 12RFRC, 15RFRC, and 17RFRC showed decreases of approximately 21.6%, 21.1%, and 20%, respectively, compared to 0RFRC. These results indicate that the addition of RSFs has an adverse effect on the elastic modulus of the concrete, and an increase in the RSF content corresponds to a decrease in EM. This reduction in EM may be attributed to various factors, such as the presence of longer RSFs in the mixture and the smaller size of the aggregates used in this study. Previous research has reported that incorporating long fibers can result in decreased EM compared to shorter fibers [45]. The other probable justification for a decline in the EM could also be that 13% of RSFs used in this study were longer than 16.5 mm because reduced EM has been reported in previous studies for the incorporation of long fibers compared to short fibers [78]. Therefore, it is important to avoid using lengthy RSFs where the elastic modulus is of prime importance. The findings highlight the importance of carefully considering the influence of RSFs on the mechanical behavior of RFRC structures. Further investigation is required to optimize the RSF content and understand the relationship between fiber characteristics and the resulting elastic modulus. These insights will contribute to the development of more sustainable and mechanically robust concrete structures.

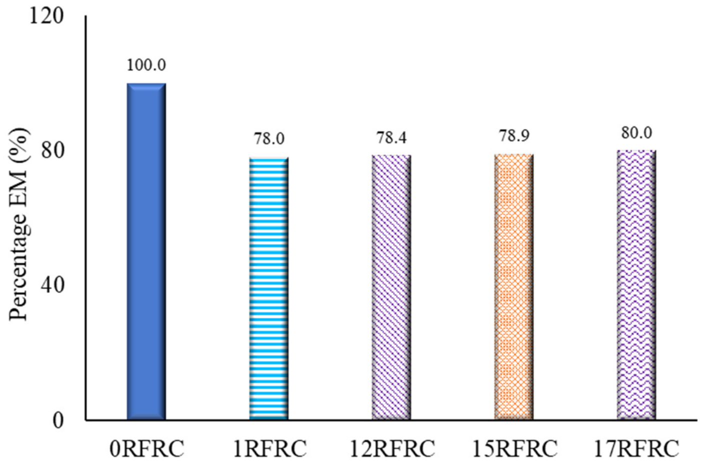

Figure 5. Percentage values of elastic modulus test.

4.4. Compression Strength Characteristics

4.4.1. Behavior under Compression Loading

The stress–strain curves for compression loading are depicted in Figure 6, illustrating the response of the specimens to increasing compression loads. Notable differences in the stress–strain behavior are observed between RFRCs and 0RFRC. RFRCs exhibited ductile behavior with smooth stress–strain responses beyond the peak load, while 0RFRC failed abruptly with brittle behavior.

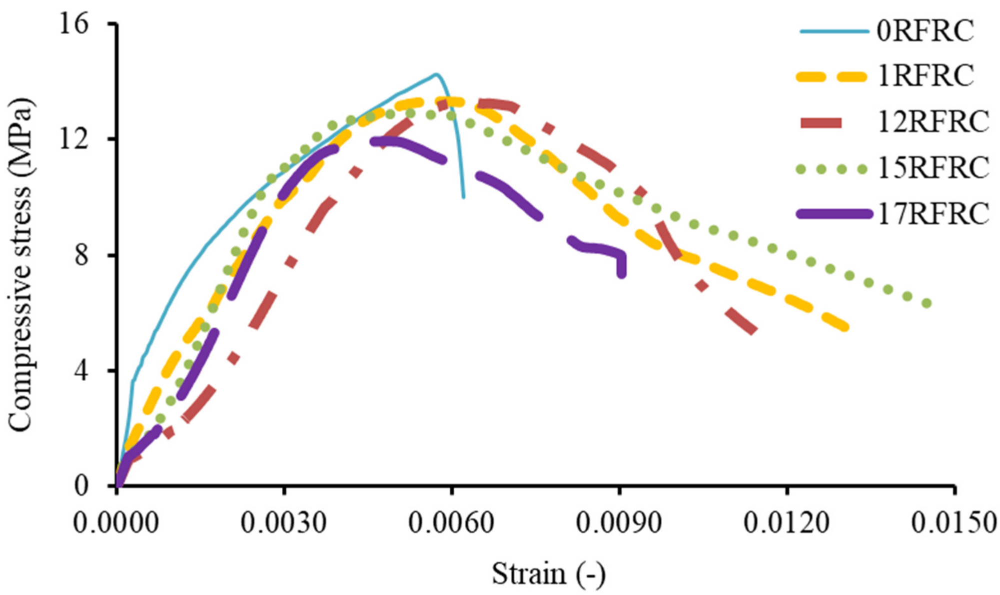

Figure 6. Curves for compression loading.

Figure 7 also provides information on the development of cracks at various stages of the loading process, including first crack initiation, peak-load cracks, and ultimate-load cracks. Cracks initiated at approximately 98–99% of the peak force for RFRCs, while 0RFRC experienced crack initiation at 98% of its peak force. The crack lengths in RFRCs were smaller compared to 0RFRC. Initial cracks in RFRCs ranged from 40 mm to 50 mm (as shown in the upper photographs of Figure 7), while crack lengths at the peak load reached 50 mm to 65 mm (as shown in the center images of Figure 7). At the final load, crack lengths extended to nearly 160 mm to 200 mm for RFRCs, as illustrated in the bottom photographs of Figure 7. RFRCs demonstrated a non-brittle failure mode, remaining intact after cracking, while 0RFRC exhibited spalling and separation along cracks. The number of cracks was higher in RFRCs, but their smaller size was advantageous for repair and grouting.

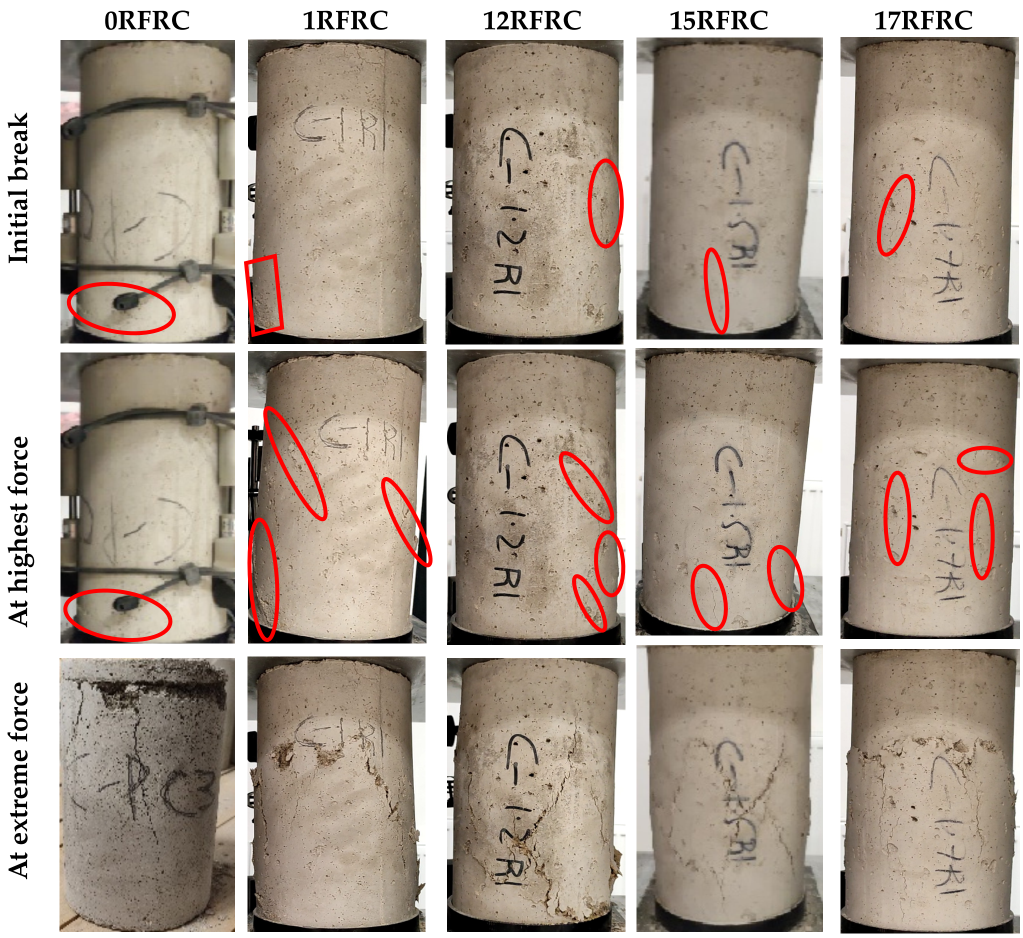

Figure 7. Specimen cracking during compression testing, the cracks observed are encircled in red.

The presence of RSFs contributed to the restraining effect and prevented complete separation along the cracks. This characteristic is advantageous for repair and rehabilitation purposes, as RFRC members, such as floors, canal-lining plates, and retaining walls, can be repaired and maintained through grouting. Conversely, 0RFRC specimens cannot be easily reconnected and repaired using simple grouting due to the separation along the cracks. Visual inspection of the RFRC specimens revealed that RSFs more than 0.80 mm thick showed releasing, while most of the thin fibers experienced both pullout and fissure. The failure of thin and long fibers was primarily attributed to fiber fracture caused by increased bond length. Similar behavior has been reported in previous studies investigating concrete incorporating less than 1% of RSF [45].

In summary, RFRCs display enhanced ductility and repairability compared to 0RFRC. The inclusion of RSFs improves the mechanical performance and integrity of concrete structures, providing opportunities for durable and resilient construction practices.

4.4.2. Compressive Test Properties

The compressive strength (CS), compression energy absorbed before the initial crack (CPE), compression postpeak energy (CCE), total energy under compressive loading (CTE), and compressive toughness index (CTI) are important properties evaluated in compression tests. The CS is determined by considering the highest compressive load. The region under the compression curve up to the stress corresponding to the initial break is taken as the CPE. The section underneath the curves from the initial crack till the final load is taken as the CPE. The entire region underneath the curve from the zero-stress to the last load is known as the CTE. The proportion of CTE to CPE is demarcated as the CTI.

The compressive strength, coefficient of variation (CoV), and cracking properties are exhibited in Table 6. The CoVs are within limits, as mentioned in other studies [79]. The CS of 17RFRC exhibited a maximum decline of 3.45 MPa as opposed to 0RFRC's CS. The CS values for 1RFRC, 12RFRC, 15RFRC, and 17RFRC are lower than that of 0RFRC, indicating a decline in compressive strength with the incorporation of RSFs. Higher doses of RSFs (more than 1%) did not positively impact the compressive strength. The highest strain values (εo) are observed for 17RFRC, indicating its ability to withstand higher strains. The CPEs reduced by 0.043 MPa for 1RFRC, 0.03 MPa for 12RFRC, 0.034 MPa for 15RFRC, and 0.05 MPa for 17RFRC than the CPE of 0RFRC. Contrasted to 0RFRC, the CCEs improved by 0.043 MPa for 1RFRC, 0.04 MPa for 12RFRC, 0.043 MPa for 15RFRC, and 0.059 MPa for 17RFRC. The fiber inclusion, which improves the after-fracture ductility, caused a rise in the CCE and CTE of RSF-reinforced specimens. The CTIs of 1RFRC, 12RFRC, 15RFRC, and 17RFRC increased by 1.22, 0.82, 1.03, and 1.76 compared to the CTI of 0RFRC. By bridging the gaps to lessen distortion, fiber insertion reduced the sizes of cracks.

Table 6. Compressive strength and related properties.

Parameters	Concrete Type				
	0RFRC	**1RFRC**	**12RFRC**	**15RFRC**	**17RFRC**
CS (MPa)	15.15	13.20	12.80	13.00	11.70
CoV * (%)	2.8	3.7	5.7	3.8	4.1
εo (-)	0.0082	0.0110	0.0116	0.0125	0.0167
C.P.E. (MPa)	0.09	0.044	0.057	0.053	0.037
C.C.E. (MPa)	0.02	0.059	0.056	0.059	0.075
C.T.E. (MPa)	0.104	0.103	0.114	0.112	0.112
C.T.I. (-)	1.2	2.40	2.00	2.21	2.94

* CoV = Coefficient of variation.

The addition of RSFs controls crack formation and spread, enhancing the CTI of RFRCs. The high dose of RSFs helps to improve the compressive toughness and postpeak energy absorption of RFRCs more than that of 0RFRC. Therefore, it can be concluded that the high dosages of RSFs (more than 1%) help enhance the concrete's postcrack energy absorption capacity and ductility under compressive loads.

Figure 8 illustrates the percentage comparison of the compression properties. RFRCs exhibited lower CS values compared to 0RFRC, with reductions ranging from 13% to 23%. The CPEs of RFRCs were lower than that of 0RFRC, while the CCEs and CTEs showed improvements. In comparison to 0RFRC, the maximum decline of 57% is noted in the CPE of 17RFRC. The CTEs of RFRCs improved, ranging from 8% to 10% compared to plain concrete. The CTIs of RFRCs were significantly higher than that of 0RFRC, with enhancements ranging from 69% to 145%. 17RFRC surpassed its counterparts in improving the CTE. The increased volume of RSF may have caused a decrease in the precrack energy absorption of RFRC relative to 0RFRC specimens. RFRCs could not control the early formation of an initial crack due to more heterogeneity and reduced CS compared to 0RFRC.

Despite the lower precrack and postcrack energies, 17RFRC exhibited the highest CTI, indicating its ability to improve toughness and postcrack resistance. RFRCs offer long-term benefits and potential cost savings in repairs compared to 0RFRC. They can be effectively utilized in applications such as side walls and concrete plates of canal linings, where joining cracked sections of plain concrete is challenging. RFRC allows simple grouting to keep cracked sections intact even after peak loads. These findings demonstrate the potential of RSFs in enhancing the after-fracture energy-absorbing capacity and toughness of RFRC subjected to compression, offering improved performance and resilience in structural applications.

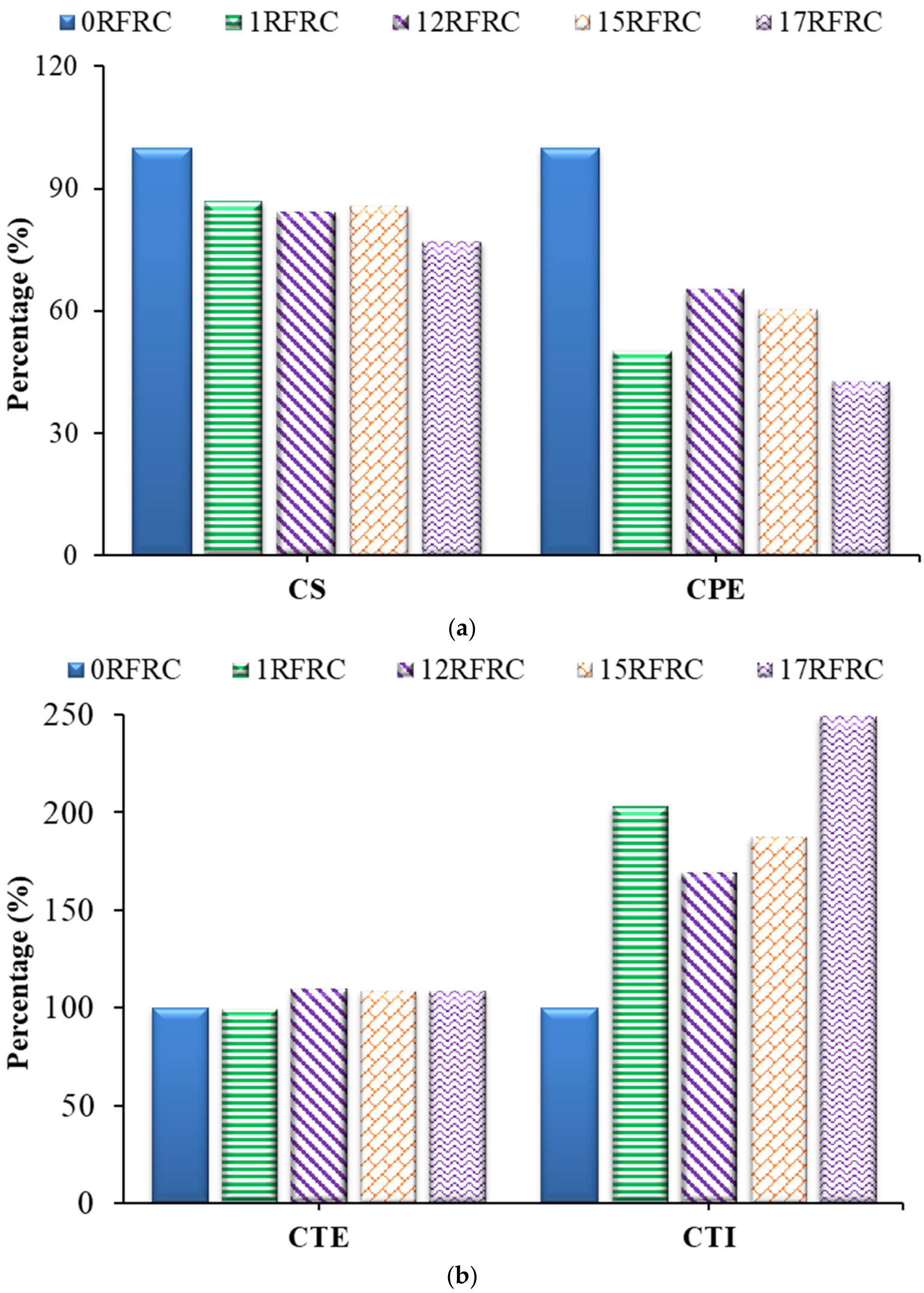

Figure 8. Percentage comparison of compressive properties (**a**) Compressive strength (CS) and precrack energy (CPE), (**b**) Total energy (CTE) and toughness index (CTI).

4.5. Split Tensile Characteristics

4.5.1. Behavior under Split Tensile Loading

The indirect tensile curves are shown in Figure 9. RFRCs exhibit a longer time to reach their peak load compared to 0RFRC, indicating increased stiffness due to the inclusion of RSFs. Figure 10 shows the cracks formed in the split tensile specimens at the three phases: at the first break, highest load, and extreme load. The first cracking is presented in the top four images of Figure 10. The initial cracking was consistent across all specimens, including 0RFRC and RSF-reinforced concrete. Less than 0.5 s span existed between the initial break and the highest load. However, RFRC specimens remained intact and connected by the fibers, while 0RFRC specimens immediately fragmented adjacent to the first crack. At the peak load, RFRCs exhibited larger crack sizes compared to 0RFRC. Figure 10′s top four photos demonstrate how the RFRCs exhibit more rise in the size of the cracks at the top load. The crack lengths at the highest and first fracture loads are approximately 140 mm for 1RFRC, 140 mm for 12RFRC, 130 mm for 15RFRC, and 100 mm for 17RFRC.

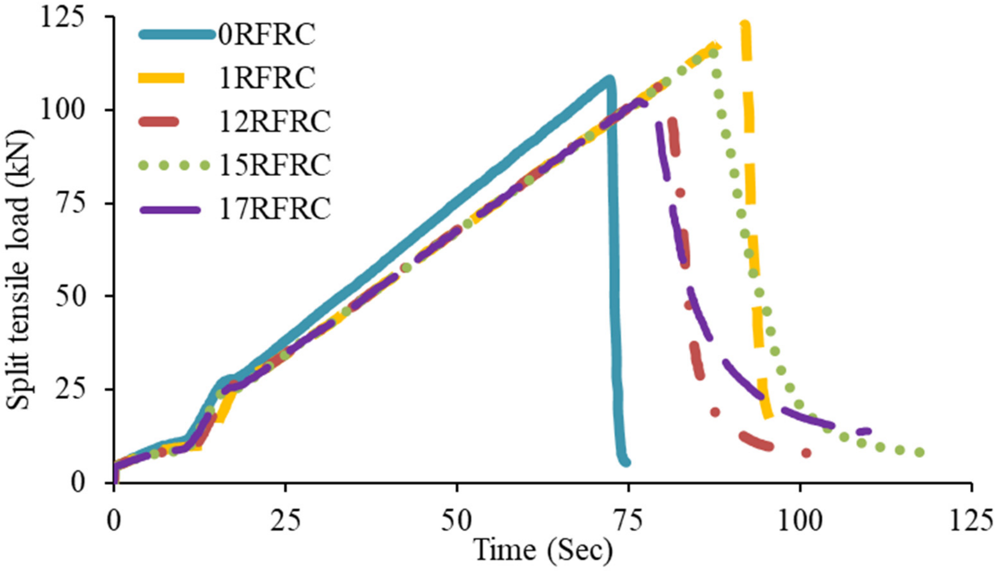

Figure 9. Split-tensile-load-versus-time curves.

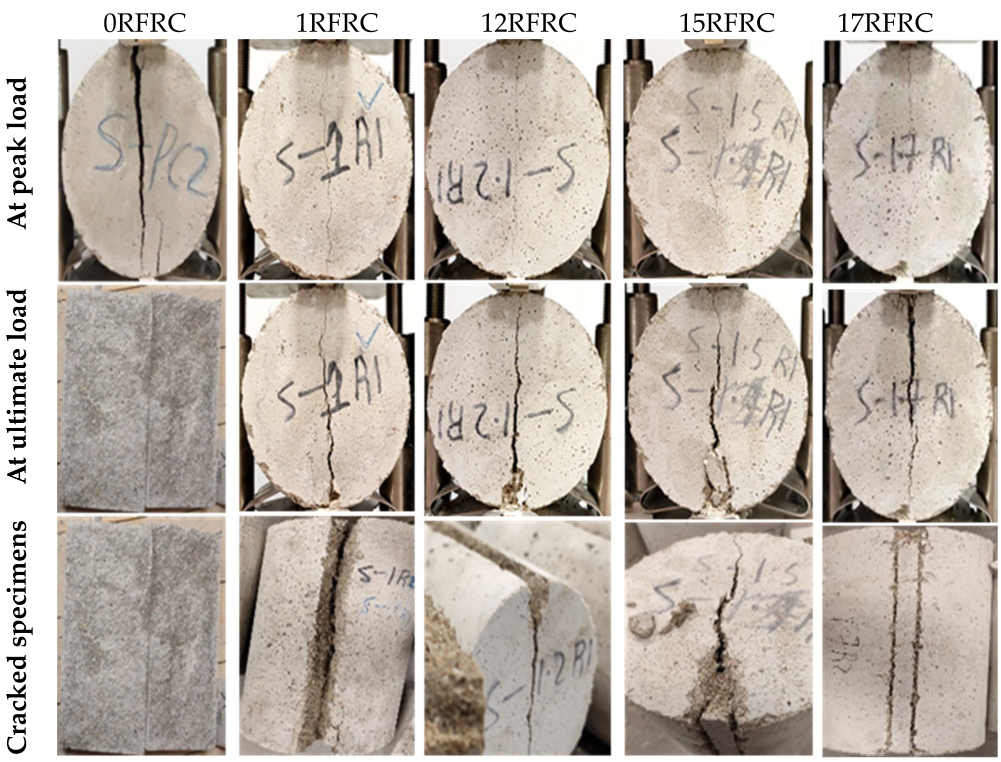

Figure 10. Crack development in the split tensile specimens.

Postcrack behavior was also observed as the test continued after reaching the highest stress. Under high stress, the crack lengths increased to the full depth for the specimens of 1RFRC, 12RFRC, 15RFRC, and 17RFRC. The broken specimens are displayed in the bottom four photographs of Figure 10. RFRC specimens, even with high doses of RSFs, remained intact and could not be separated by hand, requiring the use of a hammer. This demonstrates the strong bonding effect of the fibers in RFRC. The initial cracks in the specimens were smaller than the cracks observed at ultimate loads.

The presence of recycled tire steel fibers effectively resists crack propagation and prevents brittle failure. The physical and failure behavior of RSFs in the specimens can be observed by intentionally splitting the cylinders. Thick fibers, approximately 0.80 mm or more in diameter, exhibit a higher ratio of fiber pull-out and debonding, while shorter thick fibers show minimal fiber breakage due to their limited anchorage length across the crack. Thin fibers tend to fracture more frequently, possibly due to their shorter embedment length. It is crucial to have an equal length of fibers on both sides of the crack to fully utilize their strength. These findings highlight the ability of RSFs to enhance the crack resistance and integrity of concrete, offering potential applications to mitigate brittle failure and improve the overall durability of structures.

4.5.2. Split Tensile Strength and Associated Characteristics

The split tensile strength (SS) is determined based on the maximum split tensile load. The precrack energy (SPE) refers to the part under the split tensile curve up to the preliminary break, while the split tensile after-crack energy (SCE) represents the area from the initial crack to the maximum force. The section underneath the complete curve is used to determine the total energy (STE). The toughness index for split tensile (STI) is the ratio of STE to SPE [80].

Table 7 demonstrates the outcomes of the indirect tensile test, including the coefficients of variation (CoVs) for the split tensile strengths (SS). Compared with previous studies, the CoVs for the SS values were within the range acceptable for steel fiber-reinforced concrete [81]. Compared to 0RFRC, the SS values for 1RFRC, 12RFRC, 15RFRC, and 17RFRC showed variations. The SS of 1RFRC was 0.14 MPa more than 0RFRC. In contrast to 0RFRC, values of the SS decreased maximally for 17RFRC by 0.18 MPa, respectively.

Table 7. Split tensile strength and associated properties.

Parameters	Concrete Type				
	0RFRC	1RFRC	12RFRC	15RFRC	17RFRC
SS (MPa)	1.60	1.74	1.54	1.51	1.42
SS-CoV (%)	3.9	0.6	0.7	8.1	7.6
SPE (kN·s)	4139	5564	4160	4384	3726
SCE (kN·s)	0	501	724	820	1023
STE (kN·s)	4139	6065	4884	5204	4748
STI (-)	1.00	1.09	1.17	1.19	1.28

According to evidence from earlier experiments, adding RSFs generally improves the SS [44]. The RFRCs' SPE values also exhibit improvements compared to 0RFRC, with the highest enhancement observed in 1RFRC. However, at a high dosage of RSFs (17RFRC), the SS decreases; the SS of 17RFRC was 413 kN·s lower than that of 0RFRC. An increase in the dosage of fibers has a negative impact on shear strength; thus, precrack energy is adversely affected at more than 1.5% of RSF compared to 0RFRC. The SCE values were significantly higher for RFRCs compared to 0RFRC, indicating improved energy absorption after crack initiation. The SCE of 0RFRC was 0 kN·s because it did not sustain any load after the formation of the first crack.

A % comparison of the split tensile characteristics is shown in Figure 11. The SS of 1RFRC shows an 8% increase compared to 0RFRC, while reductions of 4%, 6%, and 11% are observed in the SS of 12RFRC, 15RFRC, and 17RFRC, respectively. The SPEs show increases for 1RFRC, 12RFRC, and 15RFRC compared to 0RFRC, with a reduction observed in 17RFRC. The STEs exhibited significant increases for all RFRCs, and the STIs demonstrated notable improvements, particularly for higher dosages of RSFs. A reduction of 10% was observed in the SPE of 17RFRC compared that of 0RFRC. The STE of 1RFRC showed a maximum increase of 47% with respect to the STE of 0RFRC. The STI of RFRC increased considerably, showing a maximum increase of 28% compared to that of 0RFRC. High doses of RSFs have proven to help improve the postcrack energy absorption of RFRCs, making them tougher than 0RFRC.

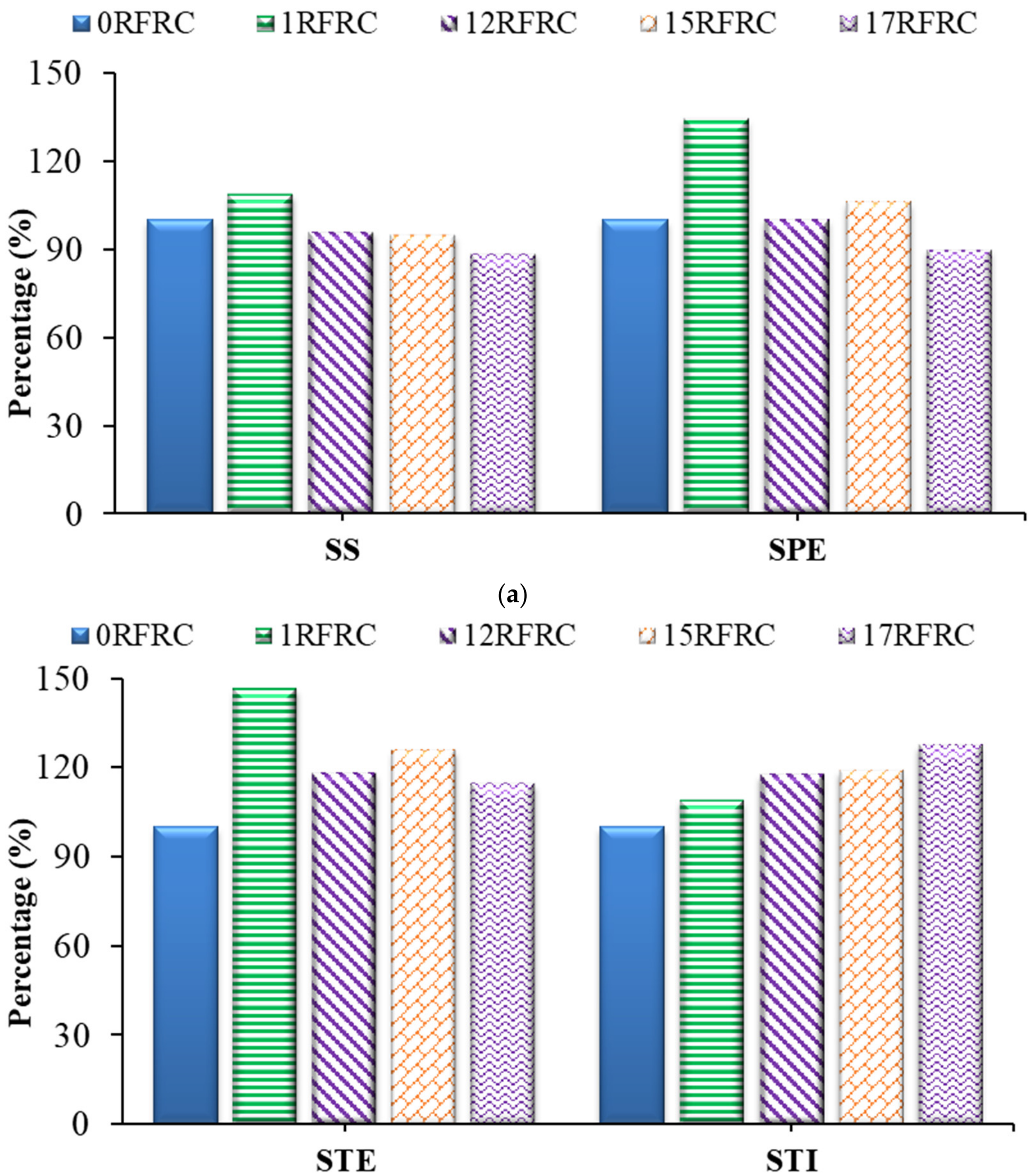

Figure 11. Comparison of split tensile properties (**a**) Split tensile strength (SS) and precrack energy (SPE), (**b**) Total energy absorbed (STE) and toughness index (STI).

In comparison to 0RFRC, the RFRC showed a substantial increase in the SCE. The STE values for RFRCs also showed an increase compared to 0RFRC, with the highest increase observed in 1RFRC. Compared to 0RFRC, the STE of 1RFRC increased by 1926 kN·s. The STI values demonstrated substantial improvements for RFRCs, indicating increased toughness and energy absorption capacity. The highest STI was observed in 17RFRC, reflecting the positive impact of a high dosage of RSFs.

According to the outcomes of split tensile testing, 1RFRC outperformed the investigated materials in improving split tensile strength and energy absorptions. Increases of 4%, 6%, and 7% were noticed in the STIs for the incorporation of 0.3%, 0.45%, and 0.75% of RSFs in concrete, compared to that of 0% RSF incorporating concrete [45]. Therefore, it can be inferred that adding a high dose of RSFs helped RFRC in improving toughness, ultimately, the mechanism to restrain the cracks better thana low-dose RSFRC. As a result of their good split tensile capabilities, RFRCs can efficiently control the fractures induced by tensile stresses. These findings indicate that the incorporation of RSFs improves the split tensile strength and energy absorption capacity of RFRCs. Among the investigated materials, 1RFRC outperformed others in terms of split tensile strength and energy absorptions. The use of a high dosage of RSFs proved more effective in enhancing toughness and crack resistance compared to a low dosage. RFRCs, with their improved split tensile capabilities, can effectively control fractures induced by tensile stresses and enhance the sustainability and service life of structures subjected to tensile cracking, such as hydraulic and marine structures. Furthermore, RFRC offers protection against severe tensile cracking that could compromise structural integrity.

4.6. Flexure Characteristics

4.6.1. Behavior under Flexure Loading

Figure 12 depicts the curves of flexural load vs. deflection for flexural beamlets. The RFRCs exhibit smoother post-crack curves, indicating improved ductility compared to 0RFRC, which shows non-ductile behavior after the peak load. The fractures formed during the three load phases are presented in Figure 13. The cracking of specimens at the initial break is demonstrated in the upper and middle pictures of Figure 13. There was less than a second between the highest and initial crack loads. The RFRC specimens demonstrated a gradual post-peak collapse, in contrast to the sudden failure observed in 0RFRC. The cracks at the peak load were wider and longer in the RFRCs.

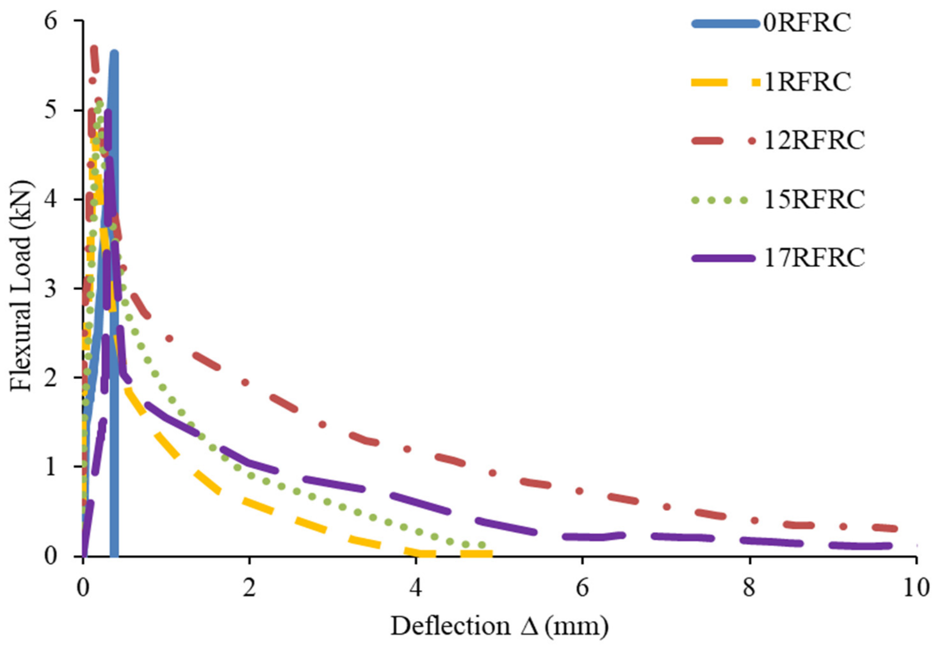

Figure 12. Load–displacement curves for flexure specimens.

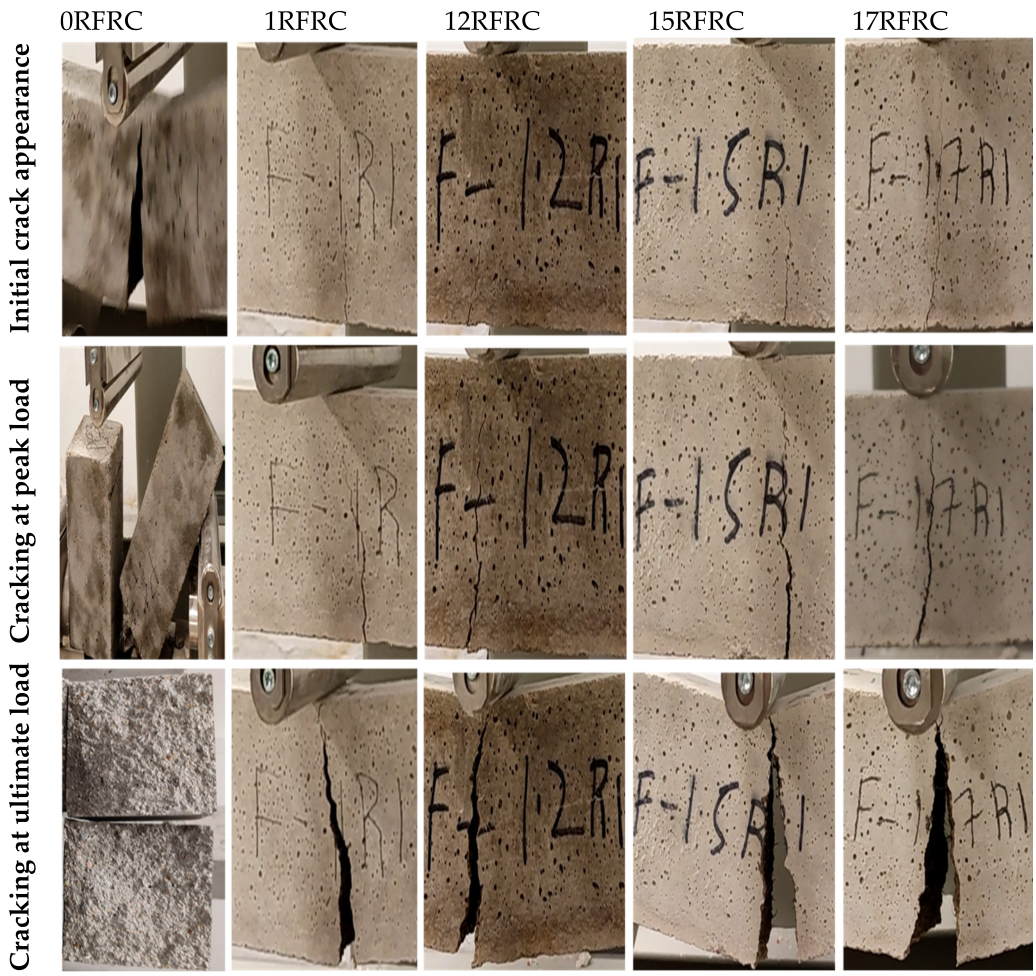

Figure 13. Crack development in the flexure specimens.

The RFRC specimens remained intact until the end of the flexure test, with some specimens showing partial detachment due to the fibers' ability to hold the sections together. The effectiveness of fibers in controlling bending cracks is influenced by their thickness and length. Thicker and longer fibers exhibit better performance in resisting bending cracks compared to short and thin fibers. High doses of fibers in the RFRCs help prevent sudden failure under flexure loading, in contrast to low doses of the same type of RSFs, which have been reported to result in sudden failure [45]. Visual inspection of the fracture surface revealed fiber breaking for long and thin fibers, while thick fibers showed higher pull-out. The probable reasons for drag-out and break of fibers in the flexure test are identical to those given for the "split tensile behavior" in the former section. In addition, the specimens showed improved MoR within the same batch for the same dose of RSFs, possessing a greater amount of fibers aligned across the crack.

It should be noted that the current study did not employ the magnetic method to align the steel fibers within the specimens during compaction. Instead, the RSFs are randomly mixed, and no special arrangements are made to align the fibers across the loading plane. However, advanced technology can be used to achieve better fiber alignment and higher strength by aligning the RSFs within the specimens during the casting stage.

4.6.2. Flexure Strength and Associated Properties

The flexure strength of the specimens is evaluated through the modulus of rupture (MoR), as per the ASTM standard [69]. The flexure strength at the deflection of 3 mm in the post-maximum load stage is taken as a residual flexure strength (RFS). The area below the flexural curve from the origin to the load at the initial fracture is known as the flexural precrack energy (FPE). Flexural cracked absorbed energy (FCE) is measured in the section between the first crack and the maximum load that lies below the flexure curve. The flexural total energy (FTE) is the area underneath the bending force–deformation curve between the zero-force and the ultimate force. The relation of FTE to FPE is considered the toughness index for flexure (FTI).

The flexure properties of prisms are shown in Table 8. The coefficients of variation are provided for MoRs. The values of MoR range from 1.71 MPa to 2.00 MPa, depending on the RSF content. A reduction of 0.20 MPa is observed in the MoRs of 1RFRC and 15RFRC compared to 0% RSF concrete, while the MoR of 12RFRC is enhanced by 0.10 MPa. The maximum MoR value of 2.00 MPa is noted for 12RFRC and 17RFRC. The FPE values range from 0.57 kN·mm to 0.68 kN·mm, with reductions observed in the RFRCs compared to 0RFRC. The FCE values range from 5.08 kN·mm to 8.71 kN·mm, indicating the increase in cracked energy absorption in RFRCs. The FTE values range from 6.18 kN·mm to 9.20 kN·mm, with significant increases observed in RFRCs compared to 0RFRC. The FTI values range from 1 to 15.02, indicating the enhanced flexure toughness of RFRCs at high doses of RSFs.

Table 8. Flexure strength and associated properties.

Parameters	Concrete Type				
	0RFRC	**1RFRC**	**12RFRC**	**15RFRC**	**17RFRC**
MoR (MPa)	1.90	1.70	2.00	1.70	1.90
MoR CoV (%)	4.1	7.3	6.0	6.5	9.5
FRS (MPa)	0	0.23	0.33	0.20	0.33
FPE (kN·mm)	1.22	0.57	0.62	0.66	0.68
FCE (kN·mm)	0.00	5.61	7.57	5.08	8.71
FTE (kN·mm)	1.22	6.18	8.19	5.75	9.20
FTI (-)	1.00	11.65	14.20	8.71	15.02

The addition of high doses of RSFs does not adversely affect the flexure energy absorption, and RFRCs maintain their crack-arresting mechanism and restriction impact. The flexure toughness indices are significantly improved in RFRCs with a high RSF content, indicating their ability to enhance post-crack behavior and energy absorption. The findings suggest that RFRCs can maintain their crack-arresting mechanism and exhibit superior performance even at higher volumetric proportions of fibers.

Figure 14 shows the percentage values of flexure test results and their comparison. A diminution of 11% is noted in MoRs for 1RFRC and 15RFRC, while a rise of 5% and 0% is noted for 12RFRC and 17RFRC compared to 0RFRC. The FPEs of 1RFRC, 12RFRC, 15RFRC, and 17RFRC were 46% to 54% smaller than that of 0RFRC. On the other hand, the FTEs of RFRCs showed significant improvements, ranging from 372% to 656% compared to 0RFRC. The FTIs experienced substantial increases of 771% to 1402% for 1RFRC, 12RFRC, 15RFRC, and 17RFRC. Notably, 17RFRC outperformed the other specimens in terms of flexure total energy and toughness. The maximum FTI of 610% and FTE of 320% were reported for using low doses (less than 1%) of RSFs [49]. Using the high dosages of RSFs boosted the flexure toughness and postcrack energy absorption further than that noticed at the low dosages of RSFs. The high doses of RSFs in RFRCs further enhanced the post-peak behavior, leading to an increase in the toughness index.

These findings demonstrate that the use of high doses of RSFs improves flexure toughness and after-crack energy beyond what was noticed with low RSF dosages [49]. Based on the improved flexural characteristics observed in this study, it is suggested that RFRCs with high doses of RSFs can effectively control cracks induced by settlement and external impact loads. Additionally, the increased RSF content enhances the ability of RFRC specimens to maintain their cracked sections together, making repairs easier compared to 0RFRC members.

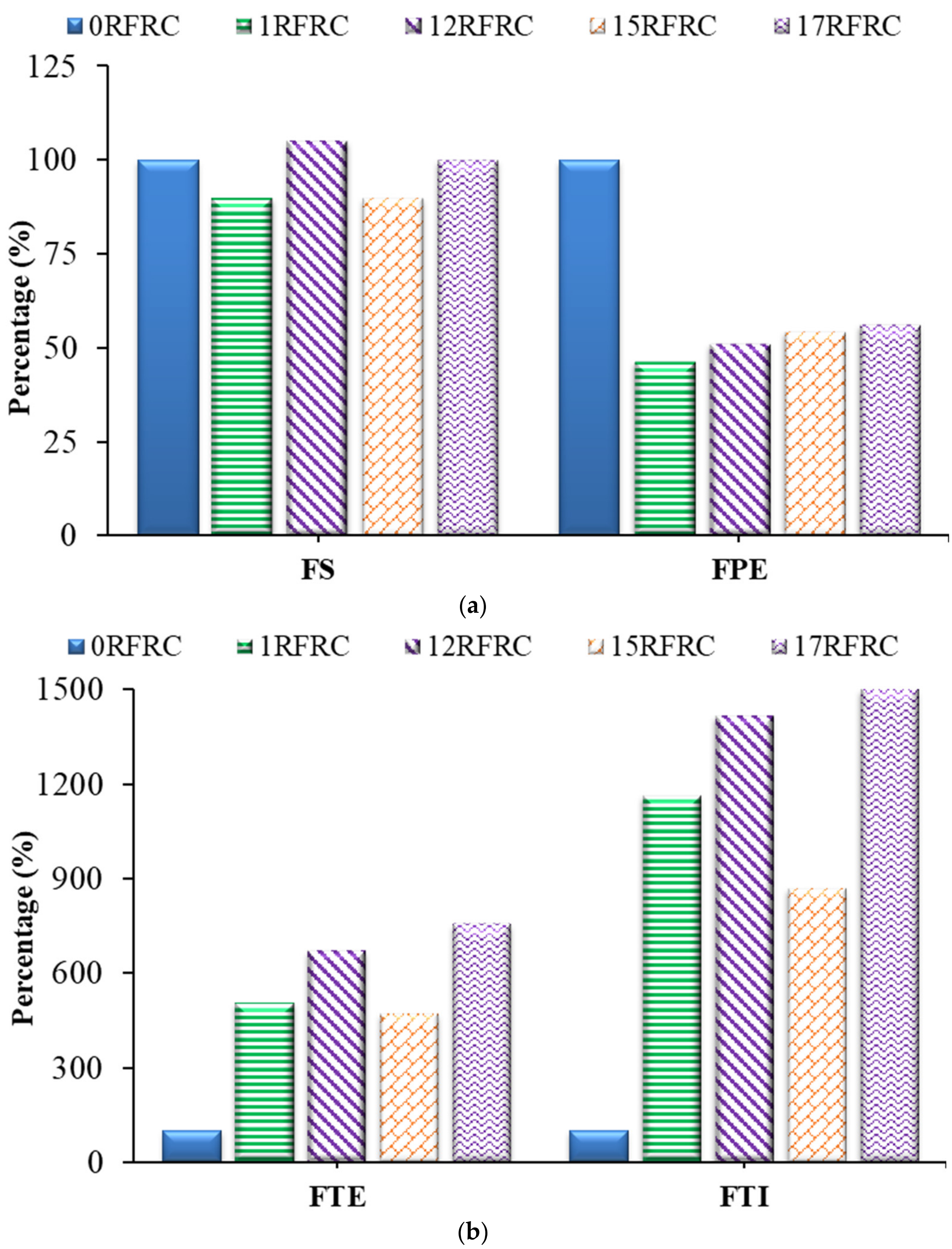

Figure 14. Comparison of flexure properties (**a**) Flexure strength (FS) and precrack energy (FPE), (**b**) Total energy absorbed (FTE) and toughness index (FTI).

5. Discussion

The evaluation of recycled tire steel fibers (RSFs) in enhancing concrete properties is a crucial aspect that merits careful examination. On the one side, the pollution burden due to secondary materials of waste tires can be decreased, and on the other side, the concrete's performance can be improved. In addition, it can help limit the use of other commercially produced fibers. This study aims to not only reduce the environmental burden associated with waste tire materials but also improve the performance of concrete. Conclusions regarding the perspective applications of RSF-reinforced concrete can be made based on the results of current experimental testing, including the strength characteristics, energy absorptions, water absorption, and linear shrinkage of RSF concrete.

5.1. RSF Versus Other Types of Fibers

By comparing RSFs with other types of fibers, such as natural, artificial, and industrial fibers, a comprehensive understanding of their respective advantages and disadvantages can be gained. Using various commercial and non-commercial fibers, including natural and artificial fibers, has been in practice for a long time in the construction industry. Natural fibers have garnered attention due to their cost-effectiveness and eco-friendly nature. Several studies have demonstrated the positive impact of natural fibers, such as jute fibers [82], sisal fibers [83], wheat straw fibers [84], bamboo fibers [85], and coconut fibers [86–89], on concrete strength properties. However, their biodegradable characteristics limit their long-term durability, while their poor resistance to water absorption hinders their effectiveness in improving concrete's longevity. Various pre-treatment methods have been explored to reduce water absorption, but these additional steps come at an added cost. Consequently, the cost-effectiveness of natural fibers is compromised when considering their long-term durability.

Artificial commercial fibers, such as nylon and glass fibers, have also shown promise in enhancing concrete properties. Notably, significant improvements in strength have been observed with the incorporation of nylon and glass fibers [90]. However, glass fibers are prone to degradation due to chemical reactions with cement, necessitating meticulous treatment to ensure their stability. This additional treatment increases the overall cost of glass fibers. Similarly, while nylon and polypropylene fibers are chemically inert and possess zero water absorption, their high cost makes them less practical for widespread use [91,92]. Together, these factors encourage the use of industrial steel fibers, But the production of industrial steel fibers also includes high costs and the generation of carbon dioxide.

In contrast, RSFs offer several notable advantages over other fiber types [59]. Firstly, RSFs are readily available at no cost, as they are derived from waste tire materials. This not only reduces the financial burden but also addresses the issue of waste disposal, contributing to environmental sustainability. Furthermore, RSFs have demonstrated a significantly lower tendency to corrode in extreme environments, ensuring the long-term durability of the reinforced concrete structures. By utilizing RSFs, the aim is to enhance concrete strength properties while mitigating the environmental impact associated with other fiber types. This research provides valuable insights into the potential use of a high dose of RSFs in the construction industry.

5.2. Leveraging RSFs for Enhancing Performance in Rigid Pavements and Other Civil Engineering Infrastructure

The current experimental results provide valuable insights into the potential applications of recycled tire steel fibers (RSFs) in the construction industry. The incorporation of high doses of RSFs showed significant improvements in flexural and split tensile strengths, with increases of 5% and 8%, respectively, compared to plain concrete (0RFRC). Furthermore, substantial enhancements were observed in toughness indices and energy for mechanical characteristics at high doses of RSFs. Notably, the total compression absorbed energy and toughness of RFRC showed maximum improvements of 10% and 149%, respectively, compared to 0RFRC. Similarly, the total split absorbed energy and split index for toughness increased by 47% and 28%, respectively. The total absorbed flexural energy and flexural index for toughness showed remarkable improvements of 656% and 1402%, respectively. Flexure strength (FS) is one of the controlling factors for the performance improvement in concrete pavements [93]. These findings suggest that RSFs have the potential to replace costly fibers in enhancing the properties of rigid pavements.

To assess the practical implications, concrete pavements designed using 0RFRC, 12RFRC, and 17RFRC were compared. The mixture type selection was based on higher flexural strength (FS) and residual flexural strength (RFS), key parameters in determining the design thickness of concrete pavements. Among the RSFRCs, 12RFRC and 17RFRC exhibited the highest FS and RFS. A jointed concrete pavement (JCP) design was employed for collector streets, utilizing bending strength, residual bending strength, and the modulus of elasticity. The pavement designs followed the ACPA method of design [94] and considered ACI 330 Traffic Spectrum C, identical subgrade conditions, and design parameters such as a 30-year design life, terminal serviceability of 2, Trucks/Day of 200, 2% growth rate of traffic, 50% directional distribution, 50% reliability, subgrade resilient modulus (MRSG) of 29 MPa, 15% slab cracking at the end of design life, and a 28 MPa subgrade reaction composite modulus with ends supported.

The design thickness for each pavement type was determined using the ACPA-approved StreetPave 12 software. Figure 15 illustrates the comparison of design thickness and material volume for JCP using three different mixtures. The design thickness for 0RFRC, 12RFRC, and 17RFRC was found to be 340 mm, 280 mm, and 290 mm, respectively. Notably, a thickness reduction of 18% can be achieved using 1.25% RSFs. Furthermore, the calculation of concrete volume required for constructing a 1 km, 3.7 m wide concrete street reveals a reduction of 448 cubic meters by incorporating 1.25% RSFs, as shown in Figure 15.

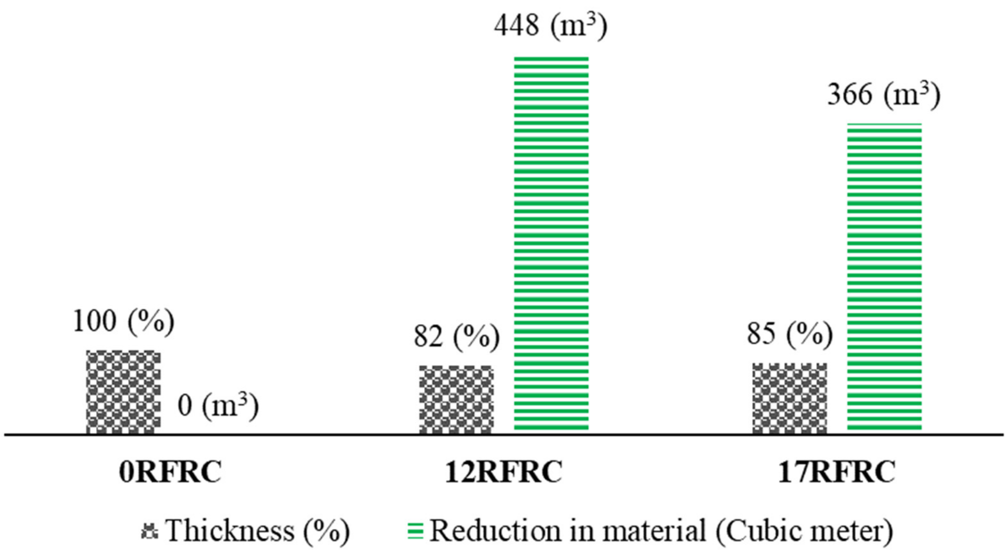

Figure 15. Reduction in the thickness (%) and materials (m^3) for 1 km of 7.32 m street.

Notably, 448 cubic meters of concrete can be reduced by using 1.25% of RSFs for constructing the same-purpose concrete pavement. This reduction in material usage positively impacts the preservation of natural resources and enhances the sustainability of the construction industry. Moreover, by using RFRC, concrete pavements can exhibit better post-cracking behavior, reducing the rate of deterioration following first fractures [93]. RSFs effectively maintain the cracked sections together, resulting in RFRC pavements with a longer usable life compared to 0RFRC pavements. Additionally, repairing cracked portions of RFRC pavements is cost-effective.

The application of RFRC can also extend to hydraulic structures, such as concrete canal linings, retaining walls, and abutments, where durability and serviceable age are critical [72]. High doses of RSFs have shown the potential to decrease the rate of deterioration caused by bending cracks and prevent severe post-cracking damage. RFRC can significantly reduce repair costs and increase the serviceable age of hydraulic structures. The mechanical property improvements and reduced linear shrinkage achieved by incorporating high doses of RSFs demonstrate their effectiveness for numerous purposes in civil engineering. In summation, the findings of our study underscore the immense environmental benefits and sustainable solutions presented by RSFs. They not only enable a substantial reduction in material usage but also minimize the need for expensive repairs, all while promoting the ethos of sustainable construction practices.

5.3. Empirical Equations

The empirical equations developed in this study provide a relationship between water absorption (WA) and the mechanical strengths of RFRC.

5.3.1. The Empirical Relation between the WA and Mechanical Strengths

Equation (1) relates WA to the cylindrical compressive strength (CS, in MPa) of the concrete, while Equation (2) relates WA (%) to the indirect tensile strength (SS, in MPa). Theoretical Equations (1) and (2) are developed using experimental data from the current study and showed good correlation with the data (R^2 = 0.58 for Equation (1) and R^2 = 0.88 for Equation (2)).

$$\mathrm{WA} = 22.63 \times CS^{-0.38} \quad (1)$$

$$\mathrm{WA} = 9.91 \times SS^{-0.29} \quad (2)$$

Figure 16 illustrates the theoretical curves generated from these empirical equations, representing the estimated relationship between WA and the corresponding strength parameters. Regression coefficients and exponents of the independent variables are optimized to obtain the best estimation of the equation. By using Equation (1) or Equation (2), it is possible to calculate the water absorption (in %) 'WA' based on the known values of CS or SS, respectively.

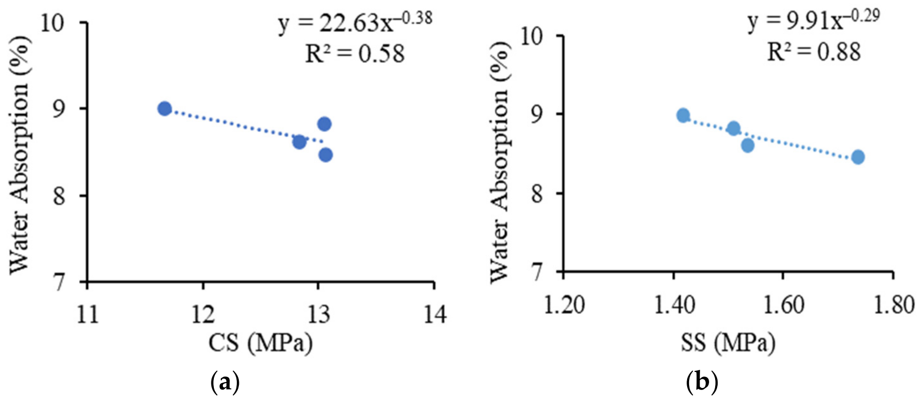

Figure 16. Development of theoretical equations for RFRC's WA (**a**) Equation (1) (**b**) Equation (2).

Table 9 shows the experimental and empirical values of WA, allowing for a comparison between the observed data and the values computed using the empirical equations. It is evident that there is a correlation between CS, SS, and WA. The relationship between CS and WA is inversely related, meaning that lower water absorption may be achieved with higher compressive strengths. On the other hand, there is an inverse relationship between WA and SS, indicating that an increase in the content of RSFs can lead to a decrease in water absorption and an increase in split tensile strength.

Table 9. Values of the WA of RFRC for empirical equations.

Property	Concrete Type			
	1RFRC	**12RFRC**	**15RFRC**	**17RFRC**
WA-Exp * (%)	8.46	8.62	8.82	9.00
WA-Emp [1] [Equation (1)] (%)	8.44	8.72	8.87	8.91
WA-Emp [1] [Equation (2)] (%)	8.45	8.75	8.79	8.96

* Experimental value of WA, [1] Empirical value of WA.

The percentage comparison of the experimental and empirically computed WAs is demonstrated in Figure 17. It can be observed that the WA values predicted by Equation (2) align more closely with the observed values compared to Equation (1). The errors associated with Equation (1) range from 0.4% to 3.4%, while Equation (2) exhibits errors ranging from 0.2% to −1.6%.

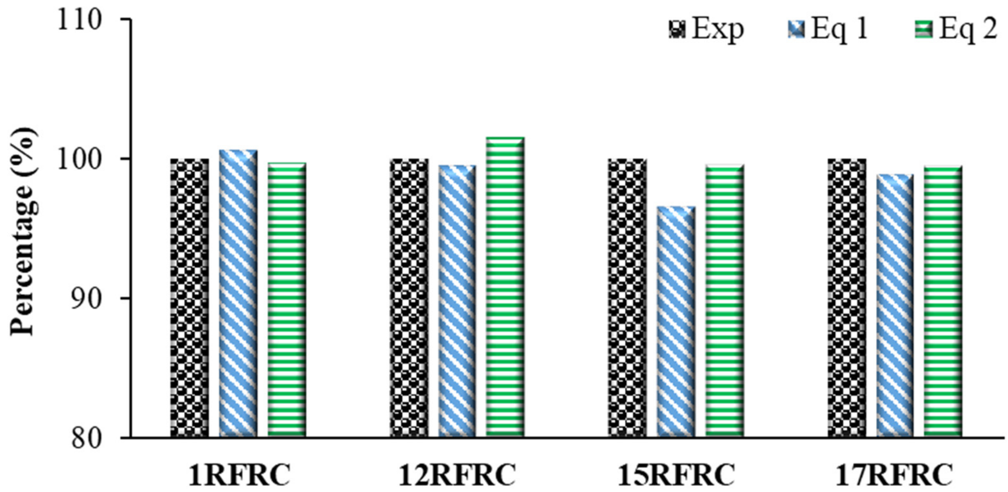

Figure 17. Percentage comparison of the WA obtained through experiments, Equations (1) and (2).

The percentage comparison of the experimental and empirically computed WAs is demonstrated in Figure 17. It can be observed that the WA values predicted by Equation (2) align more closely with the observed values compared to Equation (1). The errors associated with Equation (1) ranged from 0.4% to 3.4%, while Equation (2) exhibited errors ranging from 0.2% to −1.6%. On average, Equation (1) has an error of 1%, while Equation (2) has a slightly negative average error of −0.2%. Therefore, Equation (2) is recommended for more the accurate estimation of WA. These empirical equations serve as valuable tools for estimating water absorption in RFRC based on the concrete's mechanical strengths. By utilizing these equations, practitioners can assess the water absorption characteristics of RFRC and make informed decisions regarding its application in various construction scenarios.

5.3.2. The Empirical Correlation between the LS and Strength Properties

The empirical equations developed in this study establish a correlation between linear shrinkage (LS) and the strength properties of RFRC. Equation (3) relates LS to the cylindrical compressive strength (CS) of the concrete, while Equation (4) relates LS to the indirect tensile strength (SS). Equations (3) and (4) are as follows:

$$\mathrm{LS} = 0.07 \times CS^{-0.55} \tag{3}$$

$$\mathrm{LS} = 0.02 \times SS^{-0.55} \tag{4}$$

Figure 18 displays the empirical equations established for computing the LS. These equations were derived using experimental data and have been validated through a best-fit curve analysis, resulting in R^2 values of 0.35 and 0.89 for Equations (3) and (4), respectively. By using Equation (3) or Equation (4), it is possible to calculate the linear shrinkage (in %) based on the known values of CS or SS, respectively.

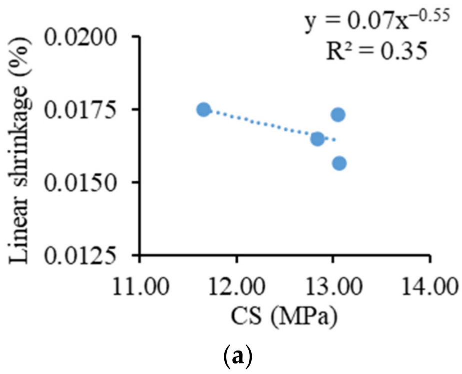

Figure 18. Development of theoretical equations for the LS of RFRCs (**a**) Equation (3) (**b**) Equation (4).

Table 10 presents the LS empirical and experimental values, allowing for a comparison between the observed data and the values computed using the empirical equations. It can be observed that the empirical LS values and experimental LS values are in acceptable agreement, indicating that the strength properties (CS and SS) have a noticeable impact on the linear shrinkage of RFRC. An inverse relationship was observed between CS or SS and LS, suggesting that incorporating RSFs in the concrete can lead to reduced linear shrinkage due to the improved compressive and split tensile strengths.

Table 10. Values of the LS of RFRC for empirical equations.

Property	**Concrete Type**			
	1RFRC	**12RFRC**	**15RFRC**	**17RFRC**
WA-Exp * (%)	0.0157	0.0165	0.0173	0.0175
WA-Emp [1] [Equation (3)] (%)	0.0170	0.0172	0.0170	0.0181
WA-Emp [1] [Equation (4)] (%)	0.0148	0.0158	0.0159	0.0165

* Experimental value of WA, [1] Empirical value of LS.

A comparison of the experimental values of LS and the empirical values of LS is shown in Figure 19. It is evident that the LS values predicted by Equation (4) closely align with the observed values, while the LS values predicted by Equation (3) deviate slightly.

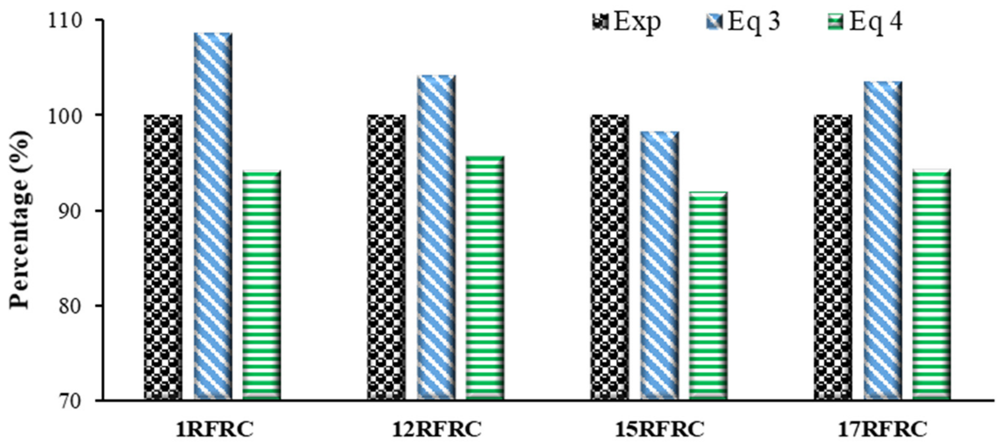

Figure 19. Percentage comparison of LS obtained through experiments, Equations (3) and (4).

The errors associated with Equation (3) range from 1.7% to −8.7%, while Equation (4) exhibited errors ranging from 4.2% to 5.7%. Considering the variations in the empirical and experimental results, Equation (4) demonstrates less than 6% variation from the experimental LS values, with a maximum deviation of 8.7% observed for Equation (3).

Therefore, it can be concluded that Equation (4) provides more accurate estimates of LS compared to Equation (3). These empirical equations serve as useful tools for estimating the linear shrinkage of RFRC based on its strength properties. By utilizing these equations, practitioners can assess the potential impact of RSFs on the concrete's shrinkage behavior and make informed decisions regarding its application in construction projects.

6. Conclusions

The experimental exploration of the impact of high percentages (ranging from 1% to 1.75%) of recycled tire steel fibers (RSF) on the strength and durability properties of concrete was a central focus of this study, driven by the goal of maximizing sustainability in concrete construction. In this research, we employed Cemix C20/25 concrete and locally sourced RSFs conforming to the EN 14889-1:2006 [58] standard from Bratislava, Slovakia. The RSFs used in their raw state contained minor rubber pieces and polyester components. This investigation also addressed the effects of these elevated RSF doses on concrete's strength and durability properties, presenting percentage comparisons of the properties under scrutiny. In essence, this study provides valuable insights into the application of high percentages of recycled tire steel fibers (RSFs) in concrete, shedding light on their impact across various properties related to concrete pavements and other civil engineering infrastructures.

Incorporating RSFs into concrete significantly affected workability, water absorption (WA), and linear shrinkage (LS). Notably, the workability, as measured by slump values, showed a substantial reduction. Simultaneously, the density of concrete only experienced a marginal decrease with a certain RSF content. The addition of RSFs resulted in increased WA, with the magnitude of this increase varying based on the RSF content. In contrast, LS exhibited a decreasing trend under the influence of RSFs, again with variations depending on the RSF content.

The introduction of high doses of RSFs significantly impacted mechanical properties, including the elastic modulus, compressive strength, and compressive strain. These findings indicate potential variations in concrete's ductility and load-bearing capabilities. Further, RSFs significantly enhanced concrete's capacity to absorb energy and toughness. The extent of these improvements varied with the specific RSF content.

Additionally, RSFs exhibited an impact on other properties like split tensile strength and flexural strength. The specific changes observed depend on the RSF content, yet they provide insights into the potential of RSFs to influence these critical mechanical attributes.

This research also highlighted the need for further study into factors like fiber diameter and impurities. The variation in RSF sizes and the presence of certain impurities, notably polyesters, influenced certain properties, emphasizing the importance of quality control in RSF usage.

Lastly, this study emphasized the cost and sustainability advantages of using RSFs in concrete pavement design. By incorporating RSFs into concrete mixtures, it is possible to reduce the design thickness compared to plain concrete, leading to significant reductions in required concrete volume for large-scale construction projects.

In conclusion, the authors have shown that this study has been instrumental in exploring the influence of RSFs on various concrete properties, contributing to a more comprehensive understanding of RSF-reinforced concrete and its potential to enhance sustainability in construction. It is now recommended to explore the influence of raw RSFs composed of a higher proportion of large-sized fibers on linear shrinkage, compared to the raw RSFs containing a similar higher proportion of small-size fibers. Further investigation into these RSF characteristics can provide valuable insights into controlling concrete's susceptibility to cracking from factors like temperature variations, freeze–thaw cycles, and wet–dry conditions. Furthermore, addressing the decrease in compressive strength observed in this study may involve exploring the potential role of raw RSFs containing only small-sized fibers in enhancing compressive strength.

Moreover, it is recommended to explore the synergistic potential of combining RSFs with other types of fibers, aiming for a comprehensive understanding of their combined effects. The proactive sorting of RSFs by size before integration is advised to minimize variations and enhance overall concrete quality. Careful consideration should be given to the use of water-absorbing polyesters to manage water absorption effectively.

Additionally, future concrete projects should consider the cost and sustainability benefits associated with RSFs, particularly in cases where reduced thickness can lead to substantial material savings and environmental advantages. This underlines the importance of collaboration between researchers and industry professionals in advancing RSF integration and driving the construction industry toward a more sustainable and efficient future.

In conclusion, this study's objectives were realized through the comprehensive exploration of RSF-reinforced concrete, offering invaluable insights for the construction industry's sustainable future.

Author Contributions: A.Z.: Conceptualization, methodology, validation, investigation, resources, data curation, writing—original draft preparation, writing—review and editing; P.Z. and I.H.: supervision, project administration, review; J.P.: testing, resources. All authors have read and agreed to the published version of the manuscript.

Funding: The National Scholarship Program of Slovakia and the Department of Concrete Structures and Bridges, Slovak University of Technology, Slovakia, are greatly appreciated for providing financial research support. In addition, the authors also acknowledge support from the National Natural Science Foundation of China (U1904177), the Excellent Youth Foundation of Henan Province of China (212300410079), and Scientific Grant Agency VEGA under contract No. VEGA1/0358/23.

Institutional Review Board Statement: Not applicable.

Informed Consent Statement: Not applicable.

Data Availability Statement: The data presented in this study are available on request from the corresponding author.

Acknowledgments: We would like to extend our heartfelt gratitude to the National Scholarship Program of Slovakia and the Department of Concrete Structures and Bridges at the Slovak University of Technology, Slovakia, for their generous financial support towards our research. Furthermore, we are thankful for the assistance of Eng. Vojtěch Uher, Technologist, ALAS, s.r.o., Slovakia in testing.

Conflicts of Interest: The authors declare no conflict of interest.

References

1. Al-Kheetan, M.J. Waste Not, Want Not: Sustainable Use of Anti-Stripping-Treated Waste Ceramic in Superpave Asphalt Mixtures. *Sustainability* **2023**, *15*, 7579. [CrossRef]
2. Al-Kheetan, M.J.; Byzyka, J.; Ghaffar, S.H. Sustainable Valorisation of Silane-Treated Waste Glass Powder in Concrete Pavement. *Sustainability* **2021**, *13*, 4949. [CrossRef]
3. Zia, A.; Khan, A.A. Effectiveness of bagasse ash for performance improvement of asphalt concrete pavements. *SN Appl. Sci.* **2021**, *3*, 502. [CrossRef]
4. Ansari, Y.; Husain, D.; Das, U.K.; Haloi, J.; Khan, N.A.; Prakash, R.; Husain, M. Ecological Footprint Assessment of Concrete: Partial Replacement of Cement by Water Treatment Sludge and Stone Dust. *Sustainability* **2023**, *15*, 7512. [CrossRef]
5. Amin, M.; Agwa, I.S.; Mashaan, N.; Mahmood, S.; Abd-Elrahman, M.H. Investigation of the Physical Mechanical Properties and Durability of Sustainable Ultra-High Performance Concrete with Recycled Waste Glass. *Sustainability* **2023**, *15*, 3085. [CrossRef]
6. Gronowicz, J.; Kubiak, T. *Recykling Zużytych Opon Samochodowych*; Wydawnictwo Naukowe Instytutu Technologii Eksploatacji—Państwowego Instytutu Badawczego: Poznan, Poland, 2007.
7. Przydatek, G.; Budzik, G.; Janik, M. Effectiveness of selected issues related to used tyre management in Poland. *Environ. Sci. Pollut. Res.* **2022**, *29*, 31467–31475. [CrossRef]
8. Godlewska, J. Recovery and Recycling of Waste Tires in Poland. *Procedia Eng.* **2017**, *182*, 229–234. [CrossRef]
9. Zhang, Y.; Zhang, Z.; Wemyss, A.M.; Wan, C.; Liu, Y.; Song, P.; Wang, S. Effective Thermal-Oxidative Reclamation of Waste Tire Rubbers for Producing High-Performance Rubber Composites. *ACS Sustain. Chem. Eng.* **2020**, *8*, 9079–9087. [CrossRef]
10. Gaska, K.; Generowicz, A.; Zimoch, I.; Ciula, J.; Siedlarz, D. A Gis Based Graph Oriented Algorithmic Model for Poly-Optimization of Waste Management System. *Arch. Civ. Eng. Environ.* **2018**, *11*, 151–159. [CrossRef]

11. European Tyre and Rubber Manufacturers' Association (ETRMA). *End of Life Tyres Management—Europe—2019*; European Tyre and Rubber Manufacturers' Association (ETRMA): Brussels, Belgium, 2021.
12. Valentini, F.; Pegoretti, A. End-of-life options of tyres. A review. *Adv. Ind. Eng. Polym. Res.* **2022**, *5*, 203–213. [CrossRef]
13. Sun, X.; Liu, J.; Hong, J.; Lu, B. Life cycle assessment of Chinese radial passenger vehicle tire. *Int. J. Life Cycle Assess.* **2016**, *21*, 1749–1758. [CrossRef]
14. European Tyre and Rubber Manufacturers' Association (ETRMA). *End of Life Tyres Management-Europe-Status*; European Tyre and Rubber Manufacturers' Association (ETRMA): Brussels, Belgium, 2018.
15. Pilakoutas, K.; Neocleous, K.; Tlemat, H. Reuse of tyre steel fibres as concrete reinforcement. *Eng. Sustain.* **2004**, *157*, 131–138. [CrossRef]
16. Evans, R.; Enne. *The Composition of a Tyre: Typical Components Creating Markets for Recycled Resources*; 21 Horse Fair: Banbury, UK, 2006.
17. Zia, A.; Ali, M. Behavior of fiber reinforced concrete for controlling the rate of cracking in canal-lining. *Constr. Build. Mater.* **2017**, *155*, 726–739. [CrossRef]
18. Farooqi, M.U.; Ali, M. Contribution of plant fibers in improving the behavior and capacity of reinforced concrete for structural applications. *Constr. Build. Mater.* **2018**, *182*, 94–107. [CrossRef]
19. Khan, M.; Ali, M. Improvement in concrete behavior with fly ash, silica-fume and coconut fibres. *Constr. Build. Mater.* **2019**, *203*, 174–187. [CrossRef]
20. Farooqi, M.U.; Ali, M. Effect of pre-treatment and content of wheat straw on energy absorption capability of concrete. *Constr. Build. Mater.* **2019**, *224*, 572–583. [CrossRef]
21. Ali, M.; Liu, A.; Sou, H.; Chouw, N. Mechanical and dynamic properties of coconut fibre reinforced concrete. *Constr. Build. Mater.* **2012**, *30*, 814–825. [CrossRef]
22. Crucho, J.; Picado-Santos, L.; Neves, J. Mechanical Performance of Cement Bound Granular Mixtures Using Recycled Aggregate and Coconut Fiber. *Appl. Sci.* **2022**, *12*, 1936. [CrossRef]
23. Mittal, M.; Chaudhary, R. Experimental Study on the Water Absorption and Surface Characteristics of Alkali Treated Pineapple Leaf Fibre and Coconut Husk Fibre. *Int. J. Appl. Eng. Res.* **2018**, *13*, 12237–12243.
24. Pawelska-Mazur, M.; Kaszynska, M. Mechanical performance and environmental assessment of sustainable concrete reinforced with recycled end-of-life tyre fibres. *Materials* **2021**, *14*, 256. [CrossRef]
25. Qin, X.; Kaewunruen, S. Environment-friendly recycled steel fibre reinforced concrete. *Constr. Build. Mater.* **2022**, *327*, 126967. [CrossRef]
26. Cerminara, G.; Cossu, R. Waste Input to Landfills. In *Solid Waste Landfilling*; Elsevier: Amsterdam, The Netherlands, 2018.
27. Mmereki, D.; Machola, B.; Mokokwe, K. Status of waste tires and management practice in Botswana. *J. Air Waste Manag. Assoc.* **2019**, *69*, 1230–1246. [CrossRef] [PubMed]
28. Vistos, L.; Galladini, D.; Xargay, H.; Caggiano, A.; Folino, P.; Martinelli, E. Hybrid industrial/recycled SFRC: Experimental analysis and design. In Proceedings of the Italian Concrete Days 2016, Rome, Italy, 27–28 October 2016; Volume 10. [CrossRef]
29. Bjegovic, D.; Baricevic, A.; Lakusic, S.; Damjanovic, D.; Duvnjak, I. Positive interaction of industrial and recycled steel fibres in fibre reinforced concrete. *J. Civ. Eng. Manag.* **2013**, *19* (Suppl. S1), S50–S60. [CrossRef]
30. Zia, A.; Zhang, P.; Holly, I.; Umar, T.; Tariq, M.A.U.R.; Sufian, M. A Comprehensive Review of Incorporating Steel Fibers of Waste Tires in Cement Composites and Its Applications. *Materials* **2022**, *15*, 7420. [CrossRef]
31. Liew, K.M.; Akbar, A. The recent progress of recycled steel fiber reinforced concrete. *Constr. Build. Mater.* **2020**, *232*, 117232. [CrossRef]
32. Merli, R.; Preziosi, M.; Acampora, A.; Lucchetti, M.C.; Petrucci, E. Recycled fibers in reinforced concrete: A systematic literature review. *J. Clean. Prod.* **2020**, *248*, 119207. [CrossRef]
33. Awolusi, T.F.; Oke, O.L.; Atoyebi, O.D.; Akinkurolere, O.O.; Sojobi, A.O. Waste tires steel fiber in concrete: A review. *Innov. Infrastruct. Solut.* **2021**, *6*, 34. [CrossRef]
34. Ahmed, H.U.; Faraj, R.H.; Hilal, N.; Mohammed, A.A.; Sherwani, A.F.H. Use of recycled fibers in concrete composites: A systematic comprehensive review. *Compos. Part B Eng.* **2021**, *215*, 108769. [CrossRef]
35. Ming, Y.; Chen, P.; Li, L.; Gan, G.; Pan, G. A comprehensive review on the utilization of recycled waste fibers in cement-based composites. *Materials* **2021**, *14*, 3643. [CrossRef]
36. Rossli, S.A.; Ibrahim, I.S. *Mechanical Properties of Recycled Steel Tire Fibres in Concrete*; Technical Report; Faculty of Civil Engineering, University Technology Malaysia: Johor Bahru, Malaysia, 2012.
37. Chen, M.; Si, H.; Fan, X.; Xuan, Y.; Zhang, M. Dynamic compressive behaviour of recycled tyre steel fibre reinforced concrete. *Constr. Build. Mater.* **2022**, *316*, 125896. [CrossRef]
38. Dehghanpour, H.; Yılmaz, K. Mechanical and impact behavior on recycled steel Fiber reinforced cementitious mortars. *Russ. J. Build. Constr. Arch.* **2018**, *3*, 67–84. Available online: https://www.researchgate.net/publication/338149695 (accessed on 25 September 2023).
39. Groli, G.; Pérez Caldentey, A.; Soto, A.G. Cracking performance of SCC reinforced with recycled fibres—An experimental study. *Struct. Concr.* **2014**, *15*, 136–153. [CrossRef]
40. Gul, A.; Alam, B.; Iqbal, M.J.; Ahmed, W.; Shahzada, K.; Javed, M.H.; Khan, E.A. Impact of Length and Percent Dosage of Recycled Steel Fibers on the Mechanical Properties of Concrete. *Civ. Eng. J.* **2021**, *7*, 1650–1666. [CrossRef]

41. Leone, M.; Centonze, G.; Colonna, D.; Micelli, F.; Aiello, M.A. Fiber-reinforced concrete with low content of recycled steel fiber: Shear behaviour. *Constr. Build. Mater.* **2018**, *161*, 141–155. [CrossRef]
42. Caggiano, A.; Folino, P.; Lima, C.; Martinelli, E.; Pepe, M. On the mechanical response of Hybrid Fiber Reinforced Concrete with Recycled and Industrial Steel Fibers. *Constr. Build. Mater.* **2017**, *147*, 286–295. [CrossRef]
43. Samarakoon, S.M.S.M.K.; Ruben, P.; Wie Pedersen, J.; Evangelista, L. Mechanical performance of concrete made of steel fibers from tire waste. *Case Stud. Constr. Mater.* **2019**, *11*, e00259. [CrossRef]
44. Skarżyński, Ł.; Suchorzewski, J. Mechanical and fracture properties of concrete reinforced with recycled and industrial steel fibers using Digital Image Correlation technique and X-ray micro computed tomography. *Constr. Build. Mater.* **2018**, *183*, 283–299. [CrossRef]
45. Zia, A.; Zhang, P.; Holly, I. Experimental investigation of raw steel fibers derived from waste tires for sustainable concrete. *Constr. Build. Mater.* **2023**, *368*, 130410. [CrossRef]
46. Shah, S.H.A.; Ali, B.; Ahmed, G.H.; Tirmazi, S.M.T.; El Ouni, M.H.; Hussain, I. Effect of recycled steel fibers on the mechanical strength and impact toughness of precast paving blocks. *Case Stud. Constr. Mater.* **2022**, *16*, e01025. [CrossRef]
47. Akhtar, T.; Ali, B.; Ben Kahla, N.; Kurda, R.; Rizwan, M.; Javed, M.M.; Raza, A. Experimental investigation of eco-friendly high strength fiber-reinforced concrete developed with combined incorporation of tyre-steel fiber and fly ash. *Constr. Build. Mater.* **2022**, *314*, 125626. [CrossRef]
48. Aiello, M.A.; Leuzzi, F.; Centonze, G.; Maffezzoli, A. Use of steel fibres recovered from waste tyres as reinforcement in concrete: Pull-out behaviour, compressive and flexural strength. *Waste Manag.* **2009**, *29*, 1960–1970. [CrossRef] [PubMed]
49. Dorr, B.J.; Kanali, C.L.; Onchiri, R.O. Shear Performance of Recycled Tyres Steel Fibres Reinforced Lightweight Concrete Beam using Palm Kernel Shear as Partial Replacement of Coarse Aggregate. *Int. J. Eng. Res. Technol.* **2019**, *12*, 1818–1823.
50. Siraj, N.; Kedir, N.S. Synthesis and characterization of pyrolised recycled steel fibers for use in reinforced concrete. *Int. J. Eng. Sci. Manag. Res.* **2017**, *4*, 21–32.
51. Köroğlu, M.A. Behavior of composite self-compacting concrete (SCC) reinforced with steel wires from waste tires. *Rev. Constr.* **2019**, *17*, 484–498. [CrossRef]
52. Abdul Awal, A.S.M.; Kadir, M.A.A.; Yee, L.L.; Memon, N. Strength and Deformation Behaviour of Concrete Incorporating Steel Fibre from Recycled Tyre. In *CIEC 2014*; Springer Nature: Singapore, 2015.
53. Centonze, G.; Leone, M.; Aiello, M.A. Steel fibers from waste tires as reinforcement in concrete: A mechanical characterization. *Constr. Build. Mater.* **2012**, *36*, 46–57. [CrossRef]
54. Younis, K.H. Mechanical Performance of Concrete Reinforced with Steel Fibres Extracted from Post-Consumer Tyres. In Proceedings of the 2nd Internationa Engineering Conference on Developments in Civil and Computer Applications, Erbil, Iraq, 22–23 November 2016.
55. Suleman, M.; Ahmad, N.; Ullah Khan, S.; Ahmad, T. Investigating flexural performance of waste tires steel fibers-reinforced cement-treated mixtures for sustainable composite pavements. *Constr. Build. Mater.* **2021**, *275*, 122099. [CrossRef]
56. Peng, G.F.; Niu, X.J.; Long, Q.Q. Experimental Study of Strengthening and Toughening for Recycled Steel Fiber Reinforced Ultra-High Performance Concrete. *Key Eng. Mater.* **2014**, *629–630*, 104–111. [CrossRef]
57. Cemix. *TECHNICKÝ LIST: Cemix Concrete Basic 25 kg, Beton 25-C20/25*; Cemix: Pöchlarn, Austria, 2022.
58. *EN 14889-1:2006*; Fibres for Concrete—Part 1: Steel Fibres—Definitions, Specifications and Conformity. European Standard Norme Europeenne Europaische Norm: Rue de Stassart, Brussels, 2006; pp. 1–26.
59. Frazão, C.; Díaz, B.; Barros, J.; Bogas, J.A.; Toptan, F. An experimental study on the corrosion susceptibility of Recycled Steel Fiber Reinforced Concrete. *Cem. Concr. Compos.* **2019**, *96*, 138–153. [CrossRef]
60. Khan, M.I.; Umair, M.; Shaker, K.; Basit, A.; Nawab, Y.; Kashif, M. Impact of waste fibers on the mechanical performance of concrete composites. *J. Text. Inst.* **2020**, *111*, 1632–1640. [CrossRef]
61. Lim, C.C.; Gowripalan, N.; Sirivivatnanon, V. Microcracking and chloride permeability of concrete under uniaxial compression. *Cem. Concr. Compos.* **2000**, *22*, 353–360. [CrossRef]
62. *ASTM C39/C39M-16*; Standard Test Method for Compressive Strength of Cylindrical Concrete Specimens. ASTM International: West Conshohocken, PA, USA, 2016.
63. *ASTM C1585-13*; Standard Test Method for Measurement of Rate of Absorption of Water by Hydraulic Cement Concretes. ASTM International: West Conshohocken, PA, USA, 2013.
64. *ASTM C143/C143M-20*; Standard Test Method for Slump of Hydraulic-Cement Contrete. ASTM International: West Conshohocken, PA, USA, 2020.
65. *ASTM C642*; Standard Test Method for Density, Absorption, and Voids in Hardened Concrete. ASTM International: West Conshohocken, PA, USA, 2013.
66. *EN 12390-13*; Testing Hardened Concrete. Part 13, Determination of Secant Modulus of Elasticity in Compression. British Standards Institution: London, UK, 2013; 13.
67. *ASTM C39/C39M-21*; Standard Test Method for Compressive Strength of Cylindrical Concrete Specimens. ASTM International: West Conshohocken, PA, USA, 2021.
68. *ASTM C496/C496M-17*; Standard Test Method for Splitting Tensile Strength of Cylindrical Concrete Specimens. ASTM International: West Conshohocken, PA, USA, 2017.
69. *ASTM C78*; Standard Test Method for Flexural Strength of Concrete. ASTM International: West Conshohocken, PA, USA, 2016.

70. *ASTM C157/C157M-17*; Standard Test Method for Length Change of Hardened Hydraulic-Cement Mortar and Concrete. ASTM International: West Conshohocken, PA, USA, 2017.
71. Khajehdehi, R.; Feng, M.; Darwin, D.; Lafikes, J.; Ibrahim, E.K.; O'Reilly, M. Combined effects of internal curing, SCMs, and expansive additives on concrete shrinkage. *Adv. Civ. Eng. Mater.* **2018**, *7*, 644–659. [CrossRef]
72. Zia, A.; Ali, M. Effectiveness of polypropylene fiber reinforced concrete in enhancement of long-term durability of hydraulic structures. In *Materials Science Forum*; Trans Tech Publications Ltd.: Baech, Switzerland, 2018; Volume 923, pp. 125–129.
73. Ramezanianpour, A.A.; Esmaeili, M.; Ghahari, S.A.; Najafi, M.H. Laboratory study on the effect of polypropylene fiber on durability, and physical and mechanical characteristic of concrete for application in sleepers. *Constr. Build. Mater.* **2013**, *44*, 411–418. [CrossRef]
74. Rostami, V.; Shao, Y.; Boyd, A.J. Durability of concrete pipes subjected to combined steam and carbonation curing. *Constr. Build. Mater.* **2011**, *25*, 3345–3355. [CrossRef]
75. Zia, A.; Zhang, P.; Holly, I. Effectiveness of hybrid discarded tire/Industrial steel fibers for improving the sustainability of concrete structures. *Constr. Build. Mater.* **2023**, *378*, 131226. [CrossRef]
76. Saje, D.; Bandelj, B.; Šušteršič, J.; Lopatič, J.; Saje, F. Shrinkage of Polypropylene Fiber-Reinforced High-Performance Concrete. *J. Mater. Civ. Eng.* **2011**, *23*, 941–952. [CrossRef]
77. Zia, A. Experimental Properties Evaluation of Fiber Reinforced Concrete Related to Canal-Lining. 2017. Available online: https://thesis.cust.edu.pk/UploadedFiles/Asad%20Zia-MCE153015.pdf (accessed on 25 September 2023).
78. Noushini, A.; Vessalas, K.; Samali, B. Static mechanical properties of polyvinyl alcohol fibre reinforced concrete (PVA-FRC). *Mag. Concr. Res.* **2014**, *66*, 465–483. [CrossRef]
79. Taghaddos, H.; Soleymani, H.R.; Robson, J.D. Precision of compressive strength testing of concrete with different cylinder specimen sizes. *ACI Mater. J.* **2010**, *107*, 461–468. [CrossRef]
80. Khan, M.; Ali, M. Effectiveness of hair and wave polypropylene fibers for concrete roads. *Constr. Build. Mater.* **2018**, *166*, 581–591. [CrossRef]
81. Marcalikova, Z.; Cajka, R.; Bilek, V.; Bujdos, D.; Sucharda, O. Determination of mechanical characteristics for fiber-reinforced concrete with straight and hooked fibers. *Crystals* **2020**, *10*, 545. [CrossRef]
82. Affan, M.; Ali, M. Experimental investigation on mechanical properties of jute fiber reinforced concrete under freeze-thaw conditions for pavement applications. *Constr. Build. Mater.* **2022**, *323*, 126599. [CrossRef]
83. Yooprasertchai, E.; Wiwatrojanagul, P.; Pimanmas, A. A use of natural sisal and jute fiber composites for seismic retrofitting of nonductile rectangular reinforced concrete columns. *J. Build. Eng.* **2022**, *52*, 104521. [CrossRef]
84. Jiang, D.; Jiang, D.; Lv, S.; Cui, S.; Sun, S.; Song, X.; He, S.; Zhang, J. Effect of modified wheat straw fiber on properties of fiber cement-based composites at high temperatures. *J. Mater. Res. Technol.* **2021**, *14*, 2039–2060. [CrossRef]
85. Bittner, C.M.; Oettel, V. Fiber Reinforced Concrete with Natural Plant Fibers—Investigations on the Application of Bamboo Fibers in Ultra-High Performance Concrete. *Sustainability* **2022**, *14*, 12011. [CrossRef]
86. Sekar, A.; Kandasamy, G. Study on durability properties of coconut shell concrete with coconut fiber. *Buildings* **2019**, *9*, 107. [CrossRef]
87. Ahmad, W.; Farooq, S.H.; Usman, M.; Khan, M.; Ahmad, A.; Aslam, F.; Al Yousef, R.; Al Abduljabbar, H.; Sufian, M. Effect of Coconut Fiber Length and Content on Properties of High Strength Concrete. *Materials* **2020**, *13*, 1075. [CrossRef] [PubMed]
88. Gu, M.; Ahmad, W.; Alaboud, T.M.; Zia, A.; Akmal, U.; Awad, Y.A.; Alabduljabbar, H. Scientometric Analysis and Research Mapping Knowledge of Coconut Fibers in Concrete. *Materials* **2022**, *15*, 5639. [CrossRef]
89. Aslam, F.; Zaid, O.; Althoey, F.; Alyami, S.H.; Qaidi, S.; Gil, J.d.P.; Martínez-García, R. Evaluating the influence of fly ash and waste glass on the characteristics of coconut fibers reinforced concrete. *Struct. Concr.* **2022**, *24*, 2440–2459. [CrossRef]
90. Khan, M.; Ali, M. Use of glass and nylon fibers in concrete for controlling early age micro cracking in bridge decks. *Constr. Build. Mater.* **2016**, *125*, 800–808. [CrossRef]
91. Durgun, M.Y.; Özen, S.; Karakuzu, K.; Kobya, V.; Bayqra, S.H.; Mardani-Aghabaglou, A. Effect of high temperature on polypropylene fiber-reinforced mortars containing colemanite wastes. *Constr. Build. Mater.* **2022**, *316*, 125827. [CrossRef]
92. Wang, C.; Wu, H.; Li, C. Hysteresis and damping properties of steel and polypropylene fiber reinforced recycled aggregate concrete under uniaxial low-cycle loadings. *Constr. Build. Mater.* **2022**, *319*, 126191. [CrossRef]
93. Hussain, I.; Ali, B.; Akhtar, T.; Jameel, M.S.; Raza, S.S. Comparison of mechanical properties of concrete and design thickness of pavement with different types of fiber-reinforcements (steel, glass, and polypropylene). *Case Stud. Constr. Mater.* **2020**, *13*, e00429. [CrossRef]
94. American Concrete Pavement Association (ACPA). Pavement Design Software, StreetPave. 2020. Available online: https://www.acpa.org/streetpave/ (accessed on 14 July 2022).